



PACKAGE DRAWING REPORT

SHEET
1 of 2

The reports and attachments generated with this sheet and listed below constitute the entire Package Drawing Report for: 2444347

These reports and attachments are and should be arranged in the following manner in order to complete the package:

NOTE: Attachment file names in parenthesis are the file names as they are in Agile .

PACKAGE CONTENTS

Placement #	Report/Attachment Name	Description	Size	Dimensions
1	BOM for Drawing REPORT FAILED		A	11 X 8.5 (Landscape)
2	{1} 2444347 a.pdf (2444347-GMI_RFI_SS15.pdf)	Print		
3	EO Report_REPORT ON GMI SPECIAL STUDY #15_ RADIO FREQUENCY INTERFERENCE_REV A_2444347.pdf	Engineering Order	A	11 X 8.5 (Landscape)

THIS SHEET IS FOR REFERENCE ONLY



Ball Aerospace
& Technologies Corp.

P.O BOX 1062
BOULDER, CO 80306

REPORT ON GMI SPECIAL STUDY #15:
RADIO FREQUENCY INTERFERENCE...

DWG
NO.

2444347

REV

A



PACKAGE DRAWING REPORT

SHEET
2 of 2

The reports and attachments generated with this sheet and listed below constitute the entire Package Drawing Report for: 2444347

The following files were located in Agile and are associated with the requested drawing, however, they have not been included in the package report. Please verify that these files do not belong in the package. Otherwise use Agile or the print report to manually correct for this.

PACKAGE EXCLUSIONS

File Name	Description	Owner
gmi_land_mask.mat	Ref - Land Mask File	Drawing
2444347-GMI_RFI_SS15_RFIDatabase.xlsx	Ref - RFI database	Drawing
2444347-GMI_RFI_SS15.docx	Native	Drawing
gmi_flag_earth_rfi.m	Ref - Matlab Code	Drawing
earth_rfi_test_file.mat	Ref - Test File	Drawing
gmi_earth_rfi_map.mat	Ref - RFI Map	Drawing
test_gmi_flag_earth_rfi.m	Ref - Test Script	Drawing

THIS SHEET IS FOR REFERENCE ONLY



Ball Aerospace
& Technologies Corp.

P.O BOX 1062
BOULDER, CO 80306

REPORT ON GMI SPECIAL STUDY #15:
RADIO FREQUENCY INTERFERENCE...

DWG
NO.

2444347

REV

A



Title Report on GMI Special Study #15: Radio Frequency Interference			Document No. 2444347	Rev A
Prepared By David Draper	Date 1/16/2015	Contract No. NNG05HY12C	CAGE Code 13993	

1 SCOPE

This report contains the results of GMI special study #15. An analysis is conducted to identify sources of radio frequency interference (RFI) to the Global Precipitation Measurement (GPM) Microwave Imager (GMI). The RFI impacts the 10 GHz and 18 GHz channels at both polarities. The sources of RFI are identified for the following conditions: over the water (including major inland water bodies) in the earth view, and over land in the earth view, and in the cold sky view. A best effort is made to identify RFI sources in coastal regions, with noted degradation of flagging performance due to the highly variable earth scene over coastal regions. A database is developed of such sources, including latitude, longitude, country and city of earth emitters, and position in geosynchronous orbit for space emitters.

A description of the recommended approach for identifying the sources and locations of RFI in the GMI channels is given in this paper. An algorithm to flag RFI contaminated pixels which can be incorporated into the GMI Level 1Base/1B algorithms is defined, which includes Matlab code to perform the necessary flagging of RFI. A Matlab version of the code is delivered with this distribution.

This special study report includes the following files:

2444347-GMI_RFI_SS15.docx: This document

2444347-GMI_RFI_SS15_RFIDatabase.docx: Spreadsheet containing significant land RFI locations

gmi_flag_earth_rfi.m: Matlab code to flag RFI over the earth

gmi_land_mask.mat: Land mask used by the algorithm

gmi_earth_rfi_map.mat: Matlab save file containing the earth RFI maps shown in this paper.

test_gmi_flag_earth_rfi.m: Test script to run gmi_flag_earth_rfi.m

earth_rfi_test_file.mat: Matlab save file used in test_gmi_flag_earth_rfi.m

In association with this report, the special study also includes the companion document and associated files:

2434007A-GMIColdRFI.docx: GMI Cold View RFI Flagging Algorithm

gmi_flag_cold_rfi.m: Matlab code to flag RFI in the cold view.

test_rfi_flag.m: Test script to run the cold sky flagging algorithm

RFI_data_all: Matlab save file used in test_rfi_flag.m

RFI_data_subset: Matlab save file used in test_rfi_flag.m

~~Export or re-export of information contained herein may be subject to restrictions and requirements of U.S. export laws and regulations, and may require advance authorization from the U.S. Government~~

Revision History, Application, and Approval are controlled by a separate database.



2 INTRODUCTION

The Global Precipitation Measurement (GPM) Microwave Imager (GMI) has been operating nearly continuously for nearly a year. The instrument is a conically scanning radiometer consisting of 13 narrow-band microwave radiometric channels with frequencies centered at 10.65 GHz, 18.7 GHz, 23.8 GHz, 36.64 GHz, 89 GHz, 166.0 GHz and 183.31 GHz. The lower frequency channel bands are maintained within the National Telecommunications & Information Administration (NTIA) allocations for “Earth Exploration-Satellite (passive).” The 10.65 GHz channel has a bandwidth of 100 MHz spanning 10.6 to 10.7 GHz. The 18.7 GHz channel has a 200 MHz bandwidth spanning 18.6 to 18.8 GHz. The NTIA-allocated bands used by GMI share utility with a number of other applications; ref. Figure 1. For example, the 100 MHz band allocated for the 10.65 GHz channel is also used for fixed ground transmissions, passive space research, and radio astronomy. It neighbors a band allocated for fixed (i.e. geosynchronous) satellite space-to-earth transmissions. Likewise, the 200 MHz 18.7 GHz band shares its allocation with fixed satellite space-to-earth transmitters. The transmitters near and around the GMI bands provide radio-frequency interference (RFI) that corrupts the GMI radiometric measurements. This paper describes a methodology for detecting RFI over ocean and land for GMI. It reports the magnitude and location of RFI for land-based transmitters and the position in geosynchronous orbit for space-based interferers.

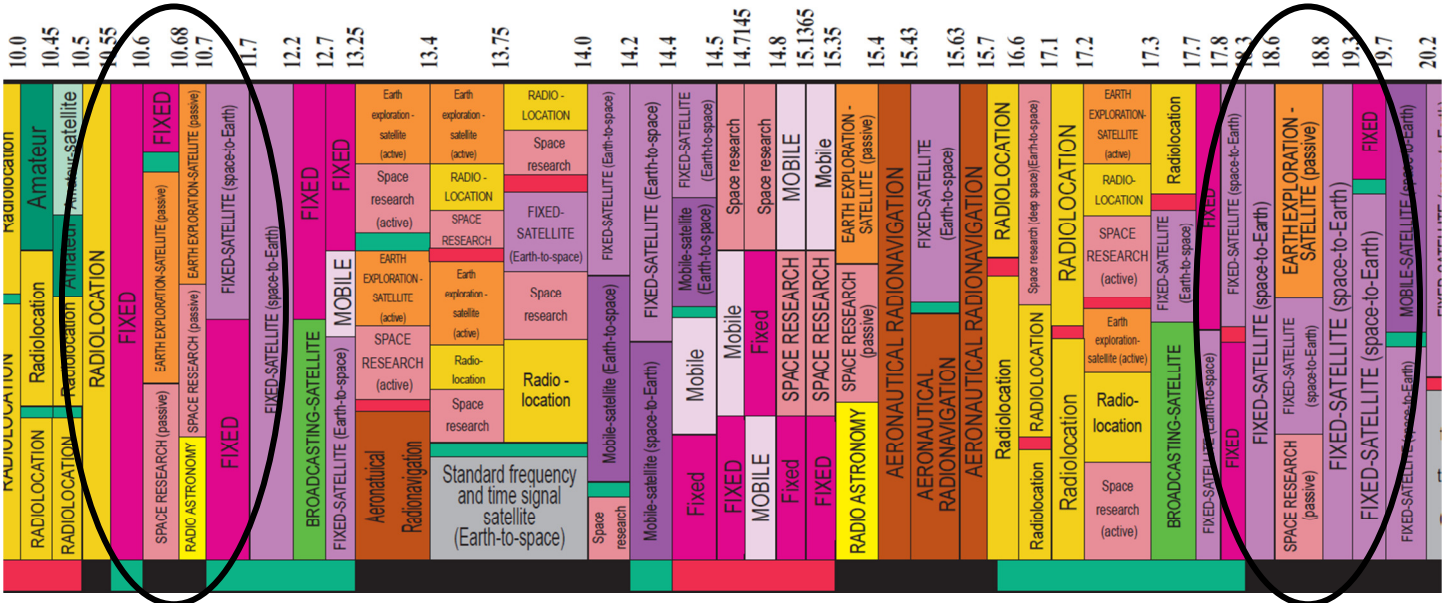


Figure 1. NTIA Spectrum allocations for the 10 and 18 GHz bands

Export or re-export of information contained herein may be subject to restrictions and requirements of U.S. export laws and regulations, and may require advance authorization from the U.S. Government



3 ANALYSIS METHODOLOGY

RFI in earth radiometric measurements produces artificially high measurements that are generally inconsistent with the natural spectral variability of the earth. A robust method of detecting RFI over land is the “spectral difference” method, where a channel of interest is compared to a neighboring channel of the same polarization. Large differences between the two channels indicate man-made transmissions. Over the ocean, RFI may be detected by comparing the ocean measurements to a model fit using a radiative transfer model. This “model difference” method may be approximated by replacing the radiative transfer model with a linear combination of other uncorrupted radiometric channels. The model difference method using other channels as proxy for the model has been successfully used on WindSat (see Li *et. al*, *TGRS*, 2006).

The spectral difference and model difference method both rely on the assumption that the other radiometric channels are sufficiently correlated with the channel of interest such that other channels may be successfully used to represent an uncorrupted version of that channel. This assumption may be used to produce a generalized RFI detection method for both land and ocean. The generalized method expands the idea of the model difference method to land scenes. For ocean and land separately, a set of coefficients is determined for the GMI 10.65 through 89 GHz channels such that the magnitude of RFI is represented as the difference between the channel of interest and a linear combination of all channels of different frequencies and their squares,

$$\Delta Tb[i] = Tb[i] - \left\{ a_o[i] + \sum_{j \in \{fc(j) \neq fc(i)\}} (a_j[i]Tb[j] + b_j[i]Tb^2[j]) \right\} \quad (1)$$

where i represents the channel index to the channel of interest and j is the channel index to all other channels with different center frequency. Eq. (1) may be written in an even simpler form, as a linear combination of all channels,

$$\Delta Tb[i] = a'_o[i] + \sum_j (a'_j[i]Tb[j] + b'_j[i]Tb^2[j]) \quad (2)$$

where j is summed over all channels, $a'_j[i]=1$ for the channel of interest, $a'_j[i]=0$ for channels with the same center frequency of the channels of interest, $a'_o[i]=-a_o[i]$, and $a'_j[i]=-a_j[i]$ for all channels (j) with a different center frequency than the channel of interest. Likewise, $b'_j[i] = 0$ for the channel of interest and all channels with the same center frequency, and $b'_j[i]=-b_j[i]$ for all other channels.

A separate set of coefficients is determined for land, ocean, and sea ice.

This methodology works well for most earth conditions. It, however, can produce false alarms along coast lines, near lakes and islands, over certain odd terrains, mis-flagged sea ice, or heavy snow. It can also be highly

~~Export or re-export of information contained herein may be subject to restrictions and requirements of U.S. export laws and regulations, and may require advance authorization from the U.S. Government~~


 Document No. 2444347 Rev. A Page 4 of 32

dependent upon geometry, and may produce anomalous results if the attitude or altitude of the spacecraft changes.

4 ALGORITHM DESCRIPTION

The RFI identification algorithm starts with identifying the type of surface viewed by the instrument. The classification relies upon a look-up table of percentage water as a function of latitude and longitude. The look-up table for the percentage land is derived from data found at <http://www.shadedrelief.com/natural3/pages/extra.html>, reduced in resolution to be more consistent with the GMI resolution with additional modification for water features not well represented in the original mask. A figure showing the water percentage look-up table is shown in Figure 2.

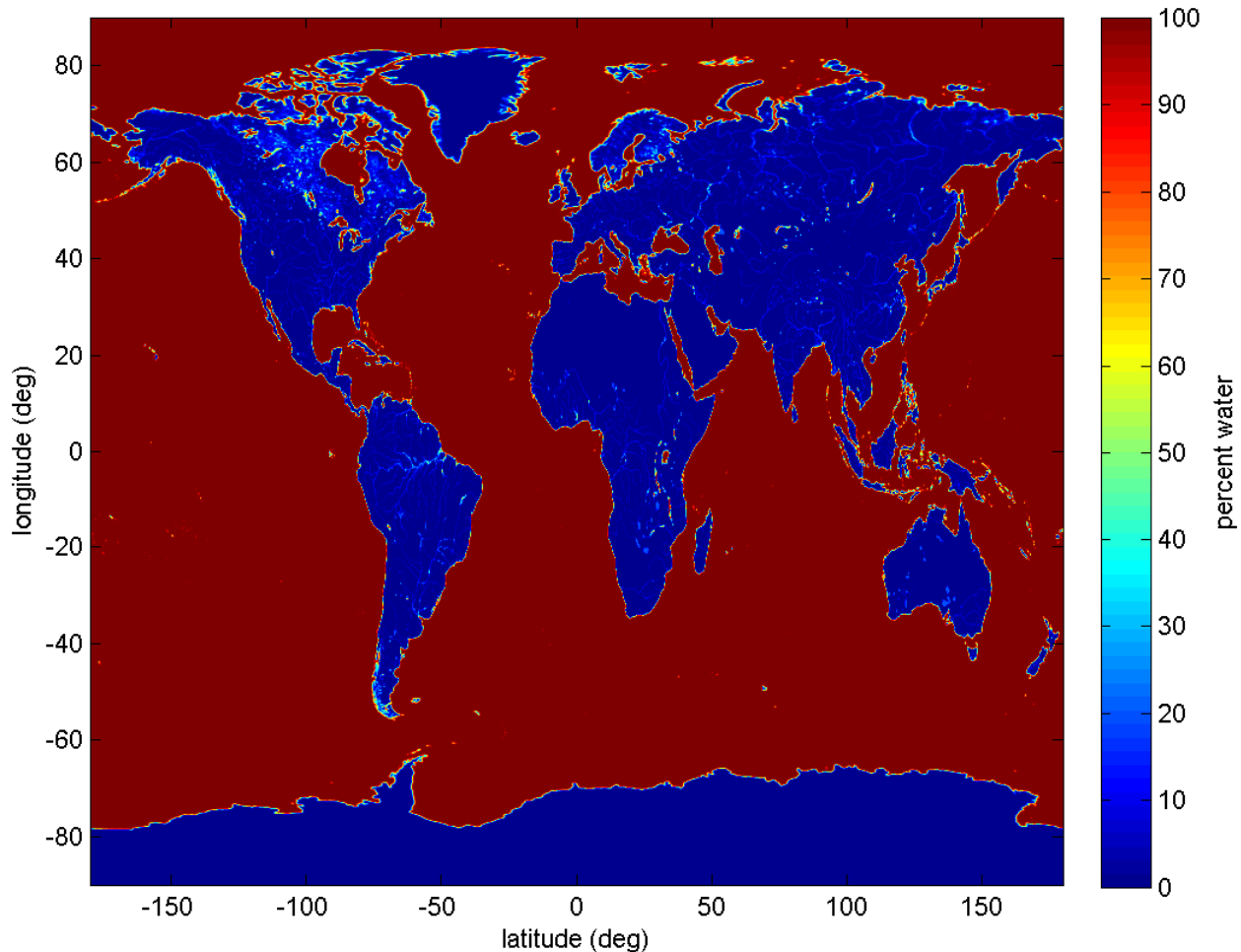


Figure 2. Percentage water for the earth. This mask is used to identify land versus ocean/lake measurements.

~~Export or re-export of information contained herein may be subject to restrictions and requirements of U.S. export laws and regulations, and may require advance authorization from the U.S. Government~~


 Document No. 2444347 Rev. A Page 5 of 32

A measurement is classified according to one of 6 surfaces if the following criteria are met:

1. Ocean/Lake: Water fraction from Figure 2 is equal to 100% (sea ice and stormy data are later removed)
2. Land: Water fraction from Figure 2 is less than 5%.
3. Coast: Water fraction is between 5% and 100%
4. Sea Ice: Measurement is flagged as Ocean/Lake AND
 Latitude is greater than 40° or less than -50° AND
 the 10 GHz H-pol channel Tb is greater than 125K.
5. Sea Ice Edge: Sea Ice is dilated by 7 cells in both along and cross-scan.
6. Stormy Seas: Measurement is flagged as Ocean/Lake AND
 36Ghz H-pol channel Tb is greater than 200K AND
 Measurement is not flagged as Sea Ice. The stormy areas are dilated by +/- 3 cells.

Any data representing stormy seas, sea ice, sea ice edge are removed from the ocean/lake classification. After identifying the surface type, the generalized RFI index $\Delta Tb[i]$ is computed as follows:

1. Ocean/Lake: Equation (2) is applied using the coefficients $a'_j[i]$ and $b'_j[i]$ computed for ocean surfaces.
2. Land: Equation (2) is applied using the coefficients $a'_j[i]$ and $b'_j[i]$ computed for land surfaces.
3. Coast: Both ocean and land coefficients are applied, and the algorithm chooses the minimum of the two. If the result is less than the coast threshold, then the algorithm sets the index equal to zero.
4. Sea Ice: Equation (2) is applied using the coefficients $a'_j[i]$ and $b'_j[i]$ computed for sea ice surfaces. If the result is less than the sea ice threshold, then the algorithm sets the index equal to zero.
5. Sea Ice Edge: The index is set to zero.
6. Stormy Seas: The index is set to zero.

The coefficients for each surface type and channel are given in appendix A.

For real-time flagging of RFI, the following $\Delta Tb[i]$ thresholds are suggested:

Table 1. Recommended thresholds for flagging RFI in a real-time algorithm

	10 GHz V	10 GHz H	18 GHz V	18 GHz H
Ocean/Lake	15K	15K	10K	10K
Land	20K / 50K*	20K / 50K*	10K / 25K*	10K / 25K*
Coast	50K	50K	30K	30K
Sea Ice	50K	50K	30K	30K
Sea Ice Edge	N/A	N/A	N/A	N/A
Stormy Seas	N/A	N/A	N/A	N/A

*Threshold for latitudes above 59 degrees and below -59 degrees latitude where heavy snow persistently exists

~~Export or re-export of information contained herein may be subject to restrictions and requirements of U.S. export laws and regulations, and may require advance authorization from the U.S. Government~~


 Document No. 2444347 Rev. A Page 6 of 32

We note that this detection method is subject to false alarms for odd or spatially varying surface characteristics. Significant surface snow will cause false alarms in both 10 and 18 GHz channels. Areas such as salt flats, widespread deserts, or mountainous terrain may also cause false alarms.

5 ANALYSIS RESULTS

The generalized RF detection method is used to evaluate RFI over first 6 months of GMI operations. Three types of RFI are found: land-based RFI detected through the GMI main beam, RFI from geosynchronous satellites reflecting off the ocean surface detected through the GMI main beam, and RFI from geosynchronous satellites interfering with the GMI cold swath.

5.1 RFI from Ground-based Transmitters

The $\Delta Tb[i]$ values are averaged over 6 months of GMI data from March 2015 through September 2015. The maximum daily average values are also computed. The average RFI index and maximum daily average RFI index plots show somewhat different characteristics of the RFI. The average RFI index tends to reduce geophysical variation and shows RFI events that are persistent over time. The maximum daily average RFI index illustrates RFI that is not terribly persistent at the cost of amplifying geophysical variation.

Figure 3 through Figure 16 show the RFI index in and around each continent except Antarctica.

The 10 GHz channels are corrupted by ground-based fixed transmitters centered in various metropolitan areas of the world. The 10 GHz RFI is especially prevalent in the Eastern Hemisphere. In the United Kingdom, Italy, Turkey and Egypt, very high levels of widespread 10 GHz RFI are detected. The 6-month average RFI levels for these areas range from 5K up to over 100K. 10 GHz RFI is also widespread in China and Japan. In the western hemisphere, the 10 GHz RFI is lower magnitude and more scattered. The highest RFI incidents in the western hemisphere occur in Mexico around cities such as Mexico City, Monterrey and Guadalajara, as well as near Sao Paulo Brazil. Please note that the "stripes" over the ocean for the 10 GHz channel are due to sun glint.

For the 18 GHz channels, RFI is detected from ground-based transmitters in several specific countries. Areas with the most 18 GHz RFI include Belarus, Libya, the Sudan, and Chile. These RFI events are generally smaller in magnitude than the 10 GHz RFI, with 6-month averages in affected areas ranging from 2K to 20K.

Appendix B provides a list of earth source RFI locations and the average RFI index over the first 6 months of GMI operation. The accompanying file `gmi_earth_rfi_map.mat` contains the data corresponding to the figures in this section.

~~Export or re-export of information contained herein may be subject to restrictions and requirements of U.S. export laws and regulations, and may require advance authorization from the U.S. Government~~

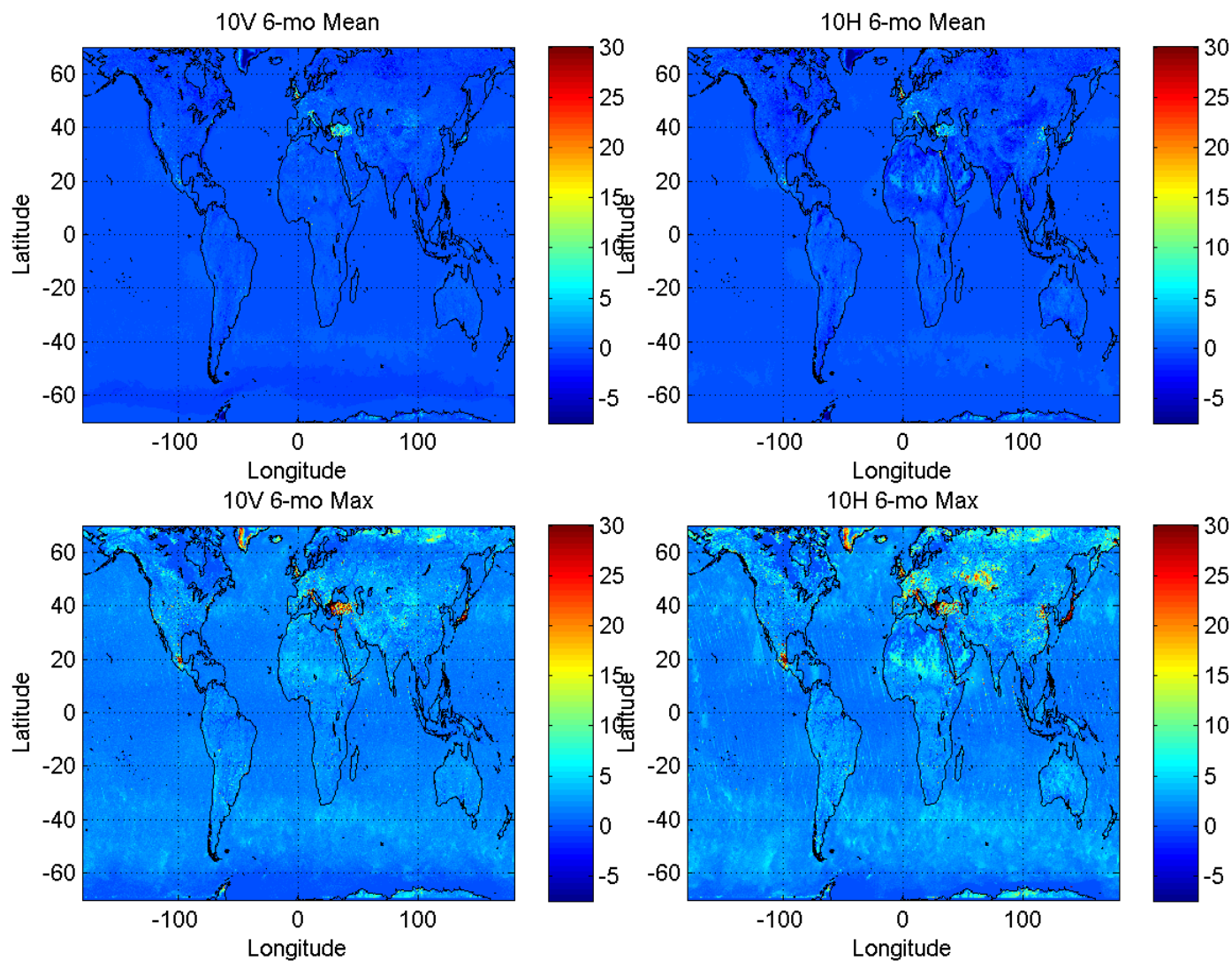


Figure 3. World-wide 10 GHz RFI index over 6 months of data from March 2014 through September 2014. Top left: average v-pol RFI index. Top right: average h-pol RFI index. Bottom left: maximum daily average v-pol RFI index. Bottom right: maximum daily average h-pol RFI index. Note that the stripes in the 10V and 10H plots over the ocean are due to sun glint.

~~Export or re-export of information contained herein may be subject to restrictions and requirements of U.S. export laws and regulations, and may require advance authorization from the U.S. Government~~

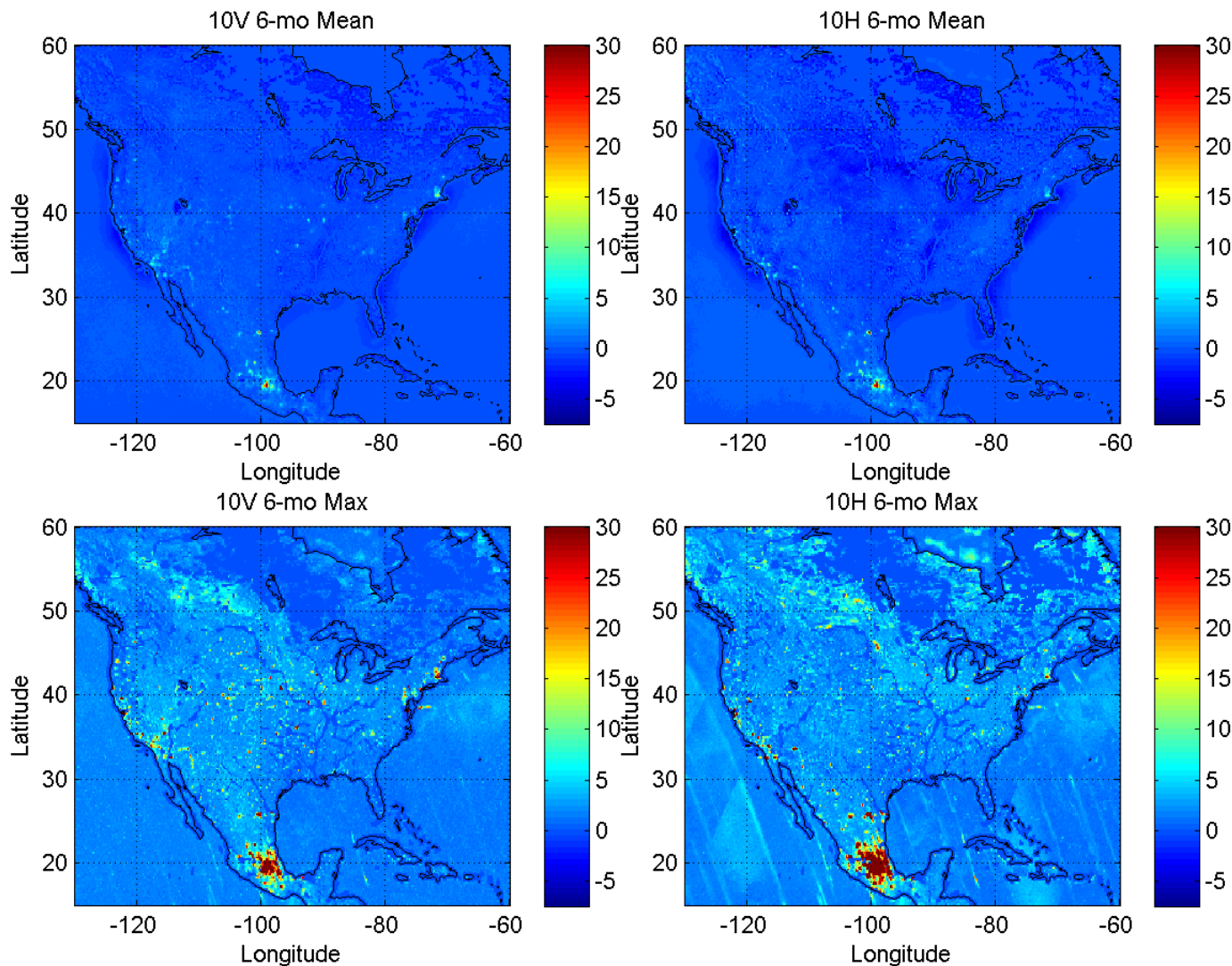


Figure 4. North America 10 GHz RFI index over 6 months of data from March 2014 through September 2014. Top left: average v-pol RFI index. Top right: average h-pol RFI index. Bottom left: maximum daily average v-pol RFI index. Bottom right: maximum daily average h-pol RFI index. RFI is exhibited in many major cities in the US, especially in California, the Midwest and New England. Mexico City and the surrounding areas show very high levels of RFI.

~~Export or re-export of information contained herein may be subject to restrictions and requirements of U.S. export laws and regulations, and may require advance authorization from the U.S. Government~~

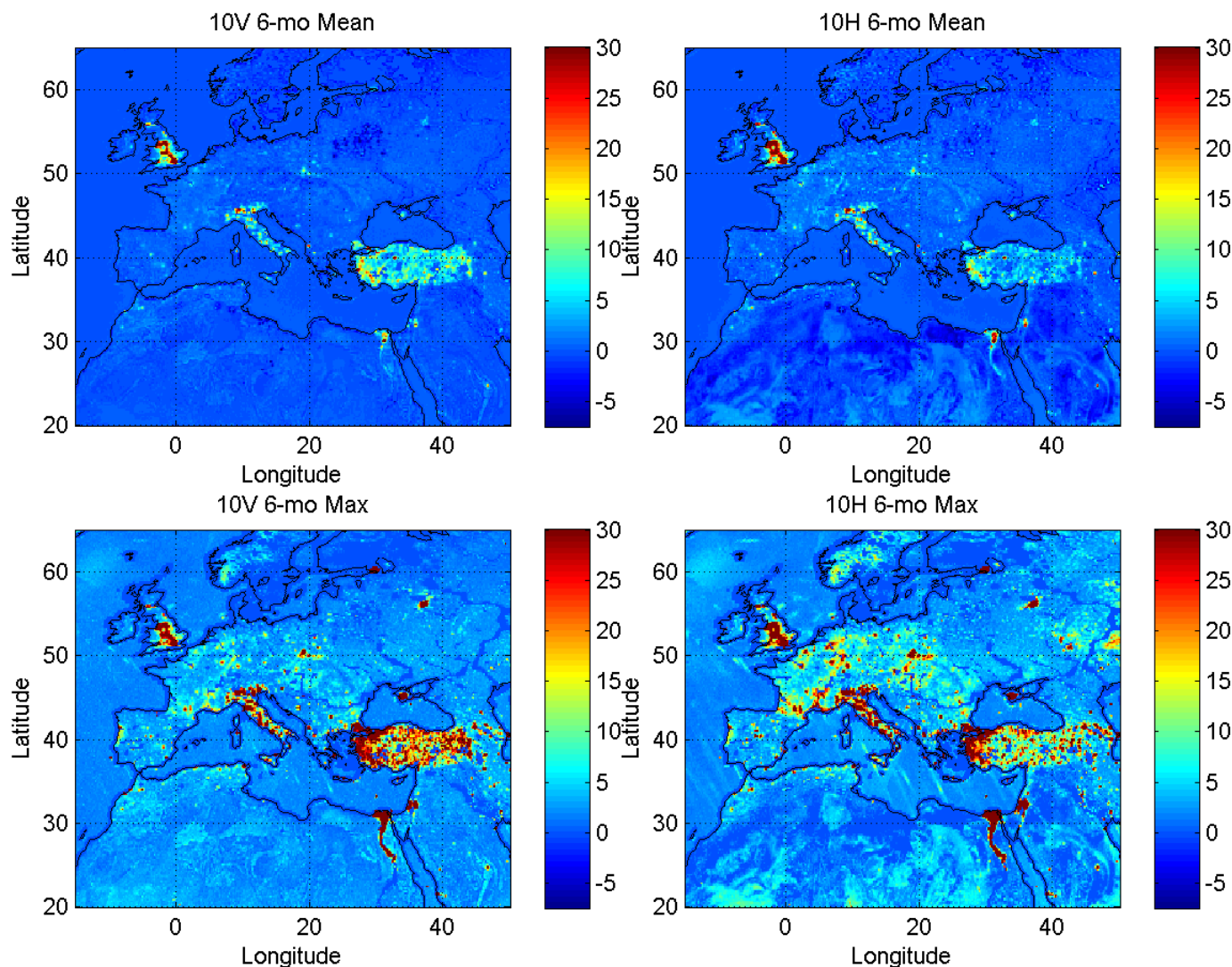


Figure 5. Europe 10 GHz RFI index over 6 months of data from March 2014 through September 2014. Top left: average v-pol RFI index. Top right: average h-pol RFI index. Bottom left: maximum daily average v-pol RFI index. Bottom right: maximum daily average h-pol RFI index. Significant RFI is noted in Great Britain, Italy, Turkey and on the Nile Delta.

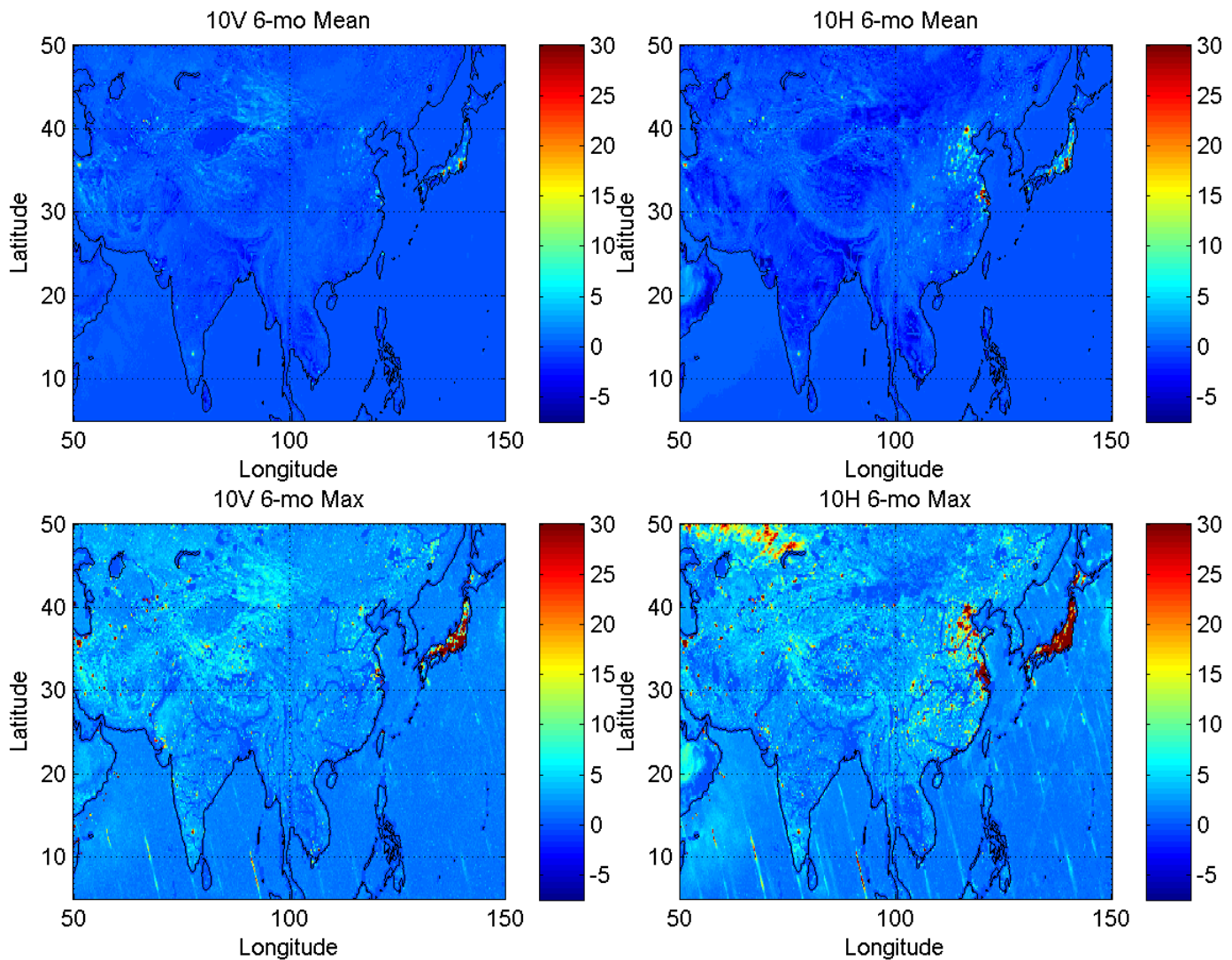


Figure 6. Asia 10 GHz RFI index over 6 months of data from March 2014 through September 2014. Top left: average v-pol RFI index. Top right: average h-pol RFI index. Bottom left: maximum daily average v-pol RFI index. Bottom right: maximum daily average h-pol RFI index. Significant RFI is shown in China and Japan. Large RFI indexes above 45 degrees latitude is due to snow in those areas.

~~Export or re-export of information contained herein may be subject to restrictions and requirements of U.S. export laws and regulations, and may require advance authorization from the U.S. Government~~

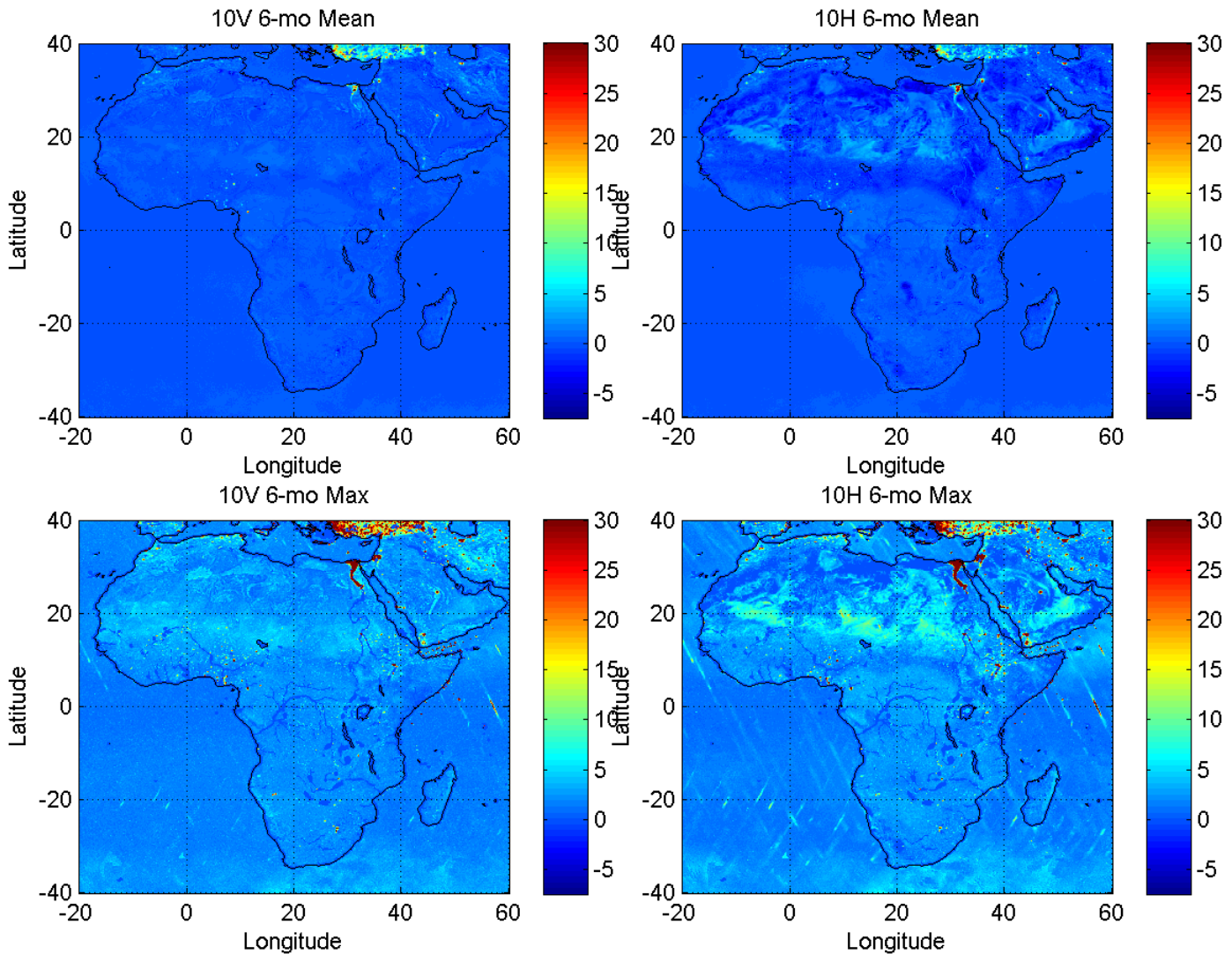


Figure 7. Africa 10 GHz RFI index over 6 months of data from March 2014 through September 2014. Top left: average v-pol RFI index. Top right: average h-pol RFI index. Bottom left: maximum daily average v-pol RFI index. Bottom right: maximum daily average h-pol RFI index. Scattered RFI is noted in Nigeria, Ethiopia, South Africa, Zambia, Tunisia, Morocco and Middle East. Ocean vessels are shown to produce RFI in the Gulf of Aden and along the west coast of Africa.

~~Export or re-export of information contained herein may be subject to restrictions and requirements of U.S. export laws and regulations, and may require advance authorization from the U.S. Government~~

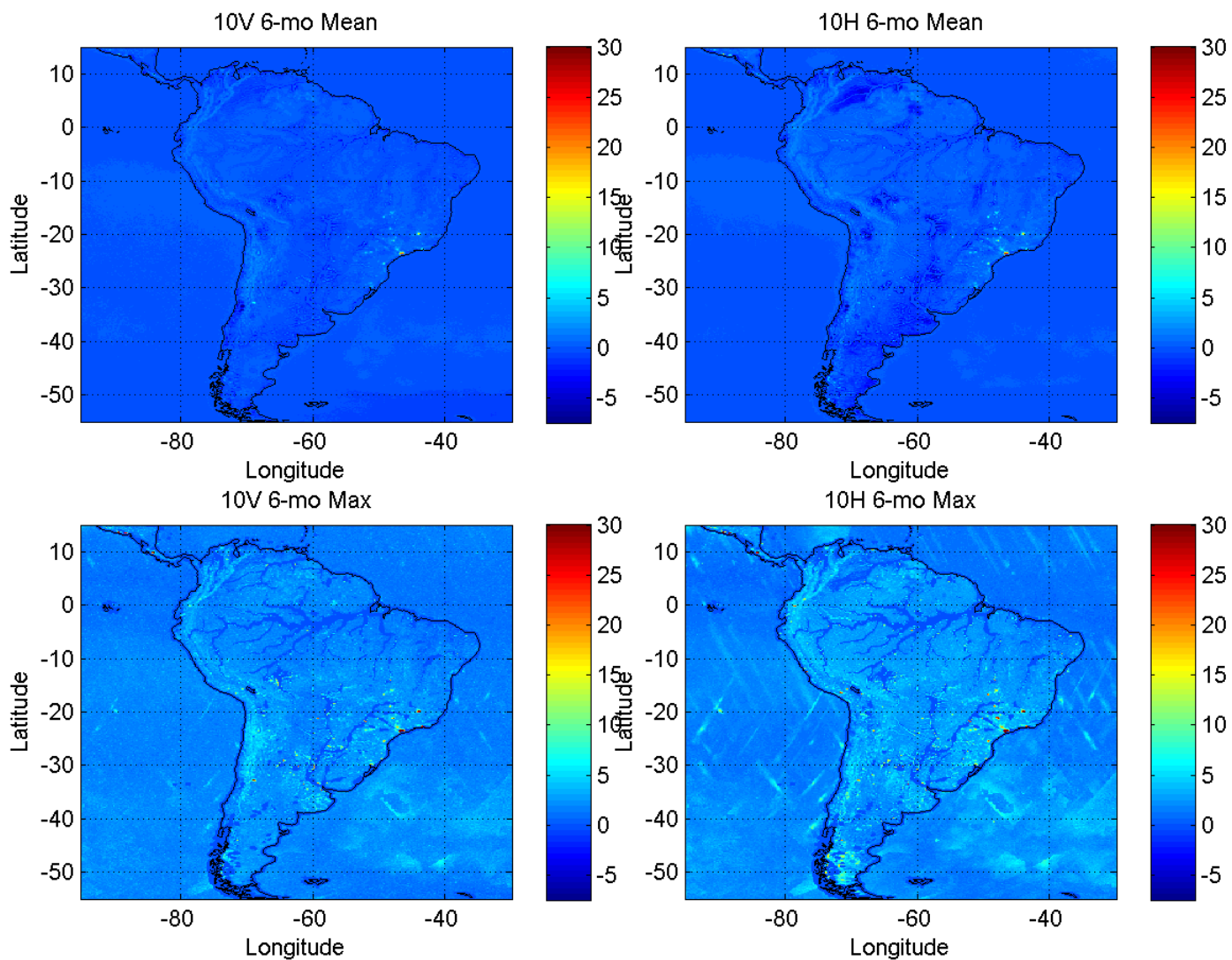


Figure 8. South America 10 GHz RFI index over 6 months of data from March 2014 through September 2014. Top left: average v-pol RFI index. Top right: average h-pol RFI index. Bottom left: maximum daily average v-pol RFI index. Bottom right: maximum daily average h-pol RFI index. RFI is shown mainly in Brazil and Argentina.

~~Export or re-export of information contained herein may be subject to restrictions and requirements of U.S. export laws and regulations, and may require advance authorization from the U.S. Government~~

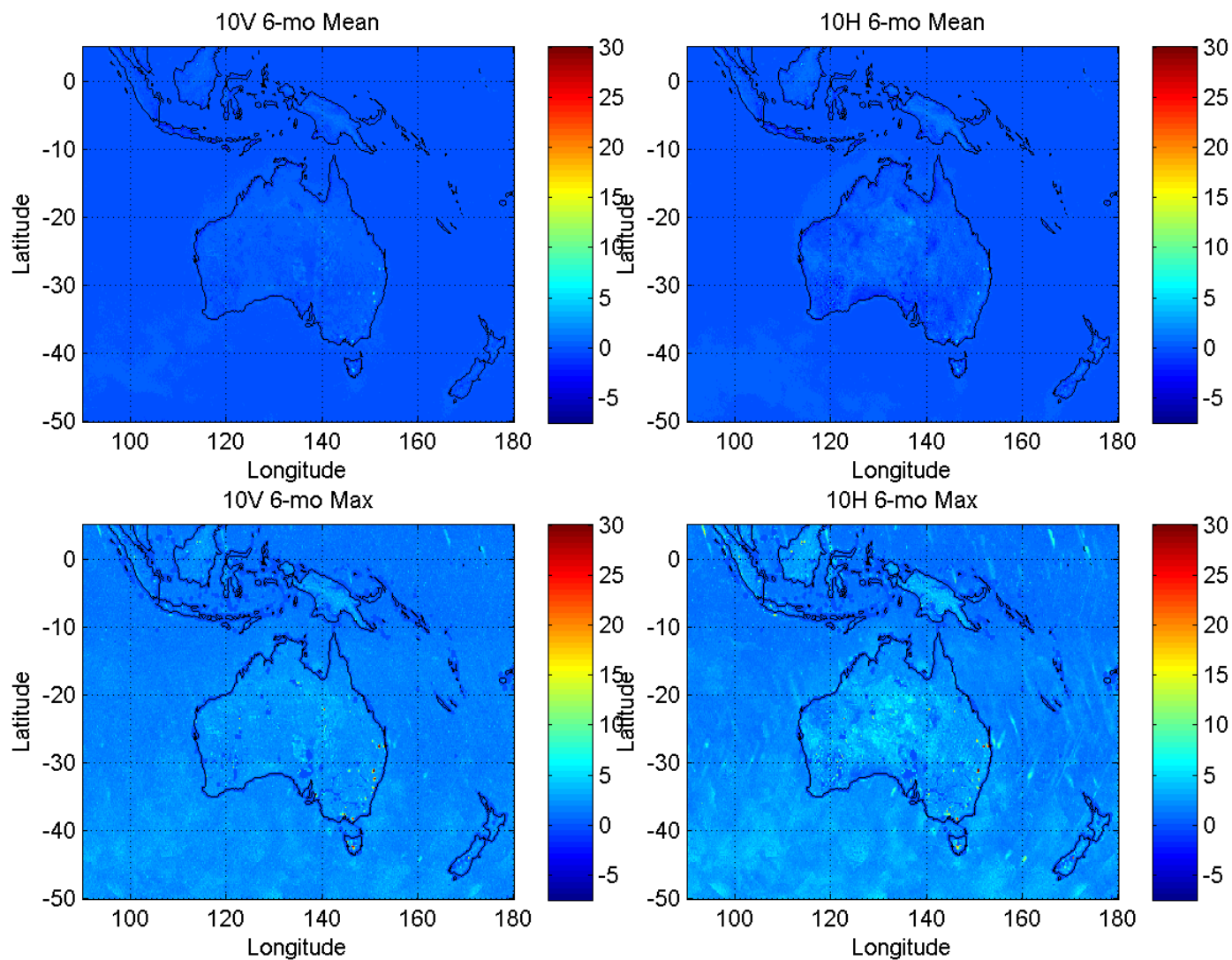


Figure 9. Australia 10 GHz RFI index over 6 months of data from March 2014 through September 2014. Top left: average v-pol RFI index. Top right: average h-pol RFI index. Bottom left: maximum daily average v-pol RFI index. Bottom right: maximum daily average h-pol RFI index. RFI is noticed along the eastern side of Australia.

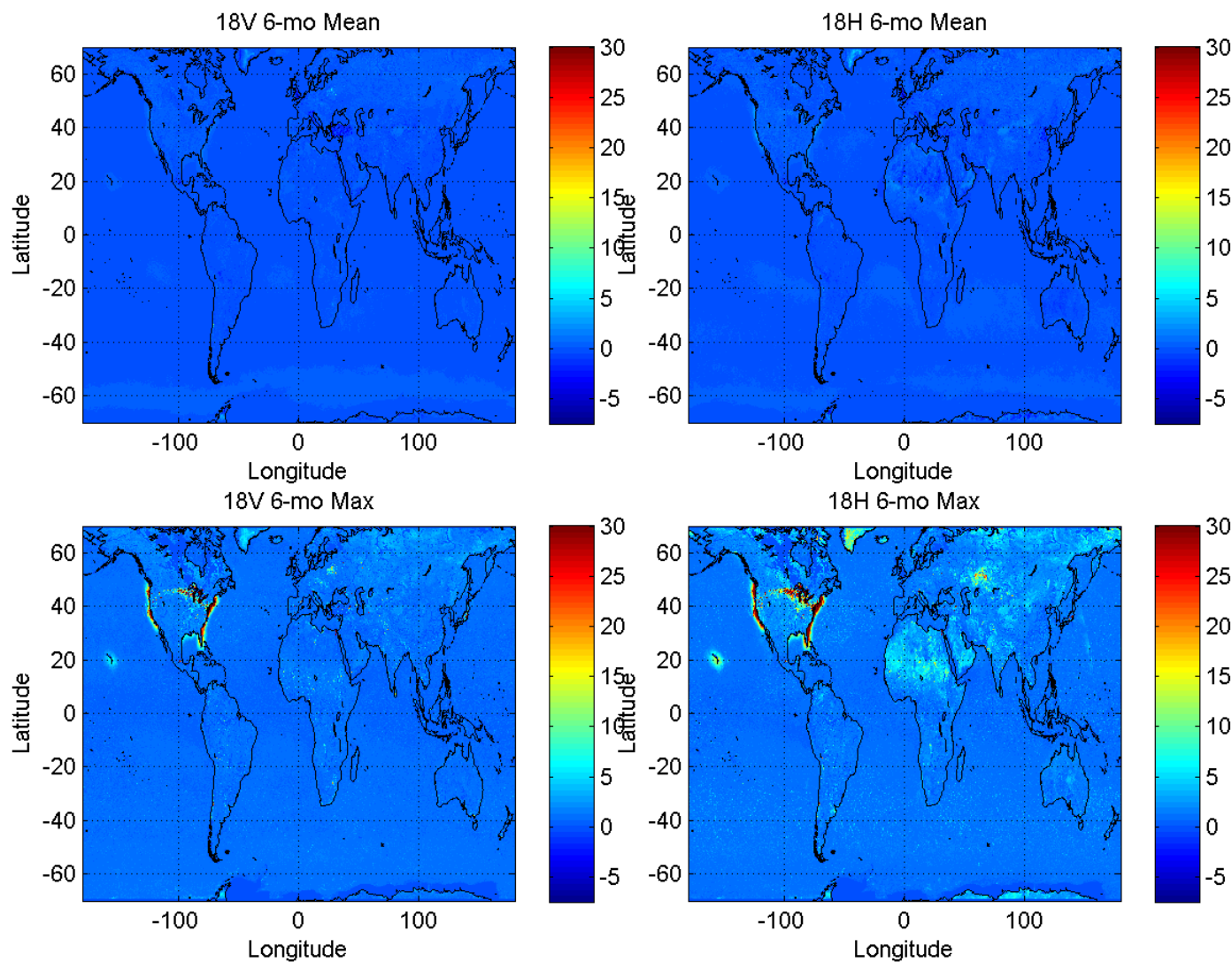


Figure 10. World-wide 18 GHz RFI index over 6 months of data from March 2014 through September 2014. Top left: average v-pol RFI index. Top right: average h-pol RFI index. Bottom left: maximum daily average v-pol RFI index. Bottom right: maximum daily average h-pol RFI index. The most noticeable RFI occurs around the continental United States and Hawaii from surface reflections from geosynchronous satellites.

~~Export or re-export of information contained herein may be subject to restrictions and requirements of U.S. export laws and regulations, and may require advance authorization from the U.S. Government~~

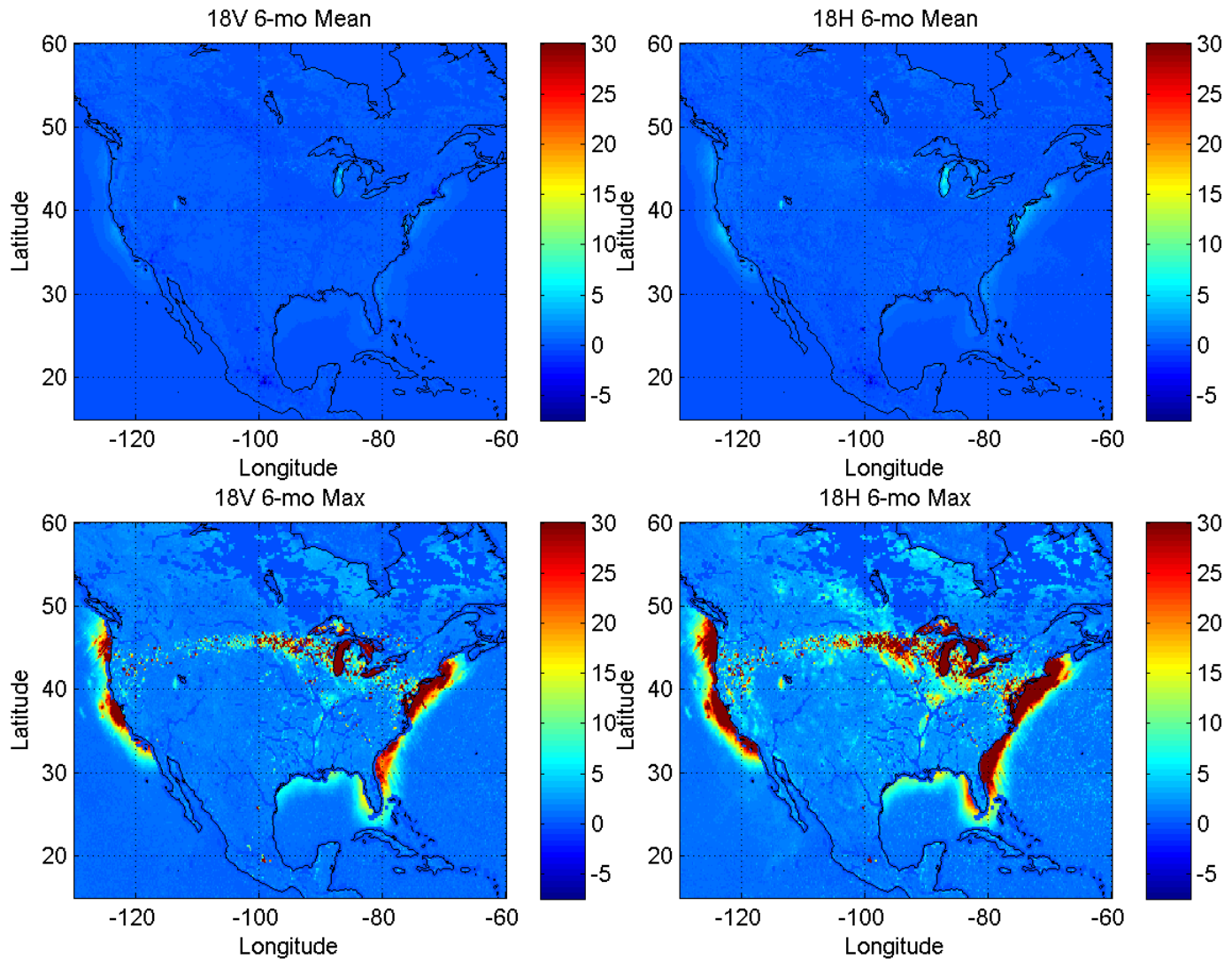


Figure 11. North America 18 GHz RFI index over 6 months of data from March 2014 through September 2014. Top left: average v-pol RFI index. Top right: average h-pol RFI index. Bottom left: maximum daily average v-pol RFI index. Bottom right: maximum daily average h-pol RFI index. Very strong RFI is noted around the continental United States from direct broadcasting satellite signals reflecting off of the oceans, Great Lakes, and other surfaces (see Section 5.3).

~~Export or re-export of information contained herein may be subject to restrictions and requirements of U.S. export laws and regulations, and may require advance authorization from the U.S. Government~~

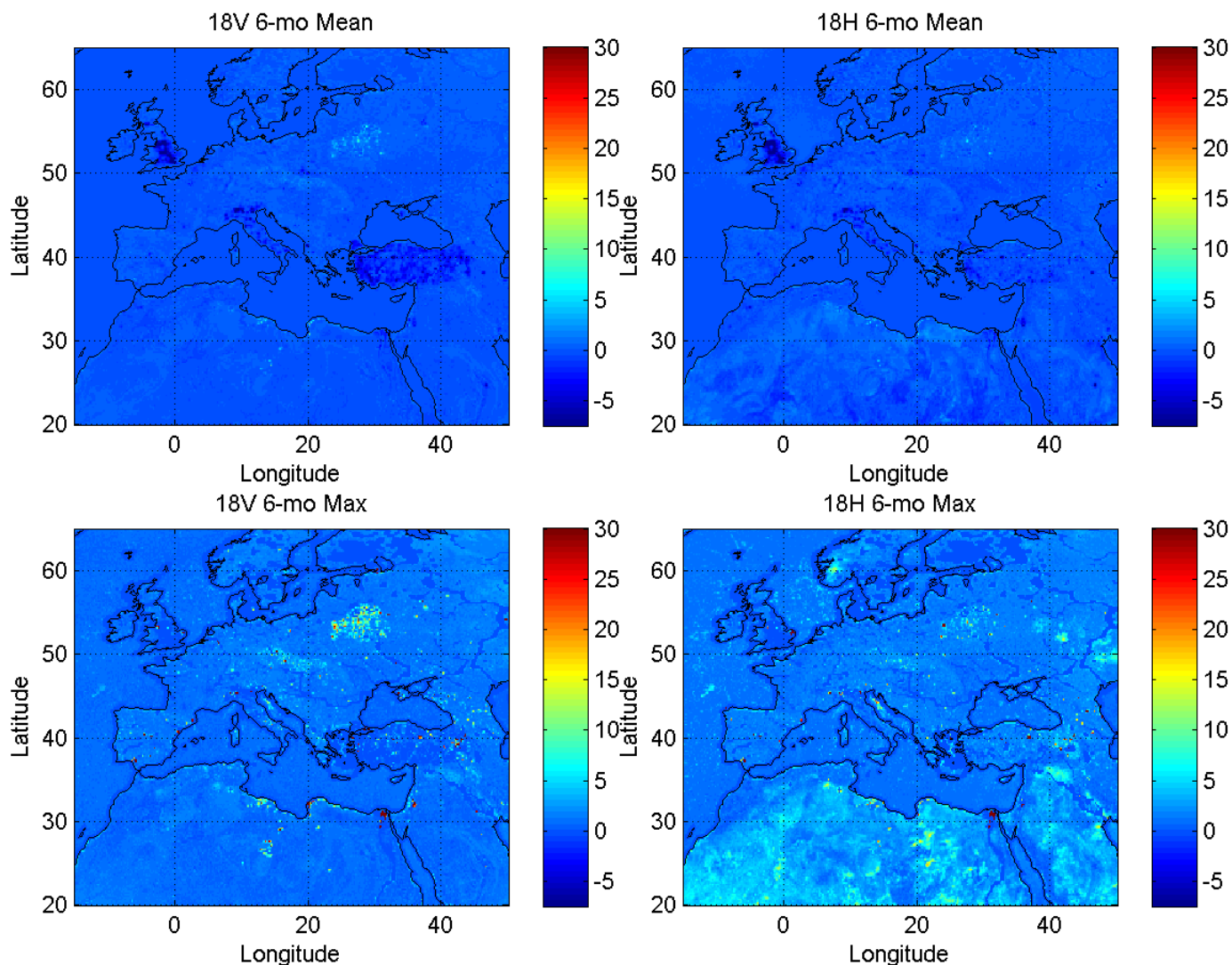


Figure 12. Europe 18 GHz RFI index over 6 months of data from March 2014 through September 2014. Top left: average v-pol RFI index. Top right: average h-pol RFI index. Bottom left: maximum daily average v-pol RFI index. Bottom right: maximum daily average h-pol RFI index. The most concentrated 18 GHz RFI occurs in Belarus, although other areas in Europe show scattered RFI as well.

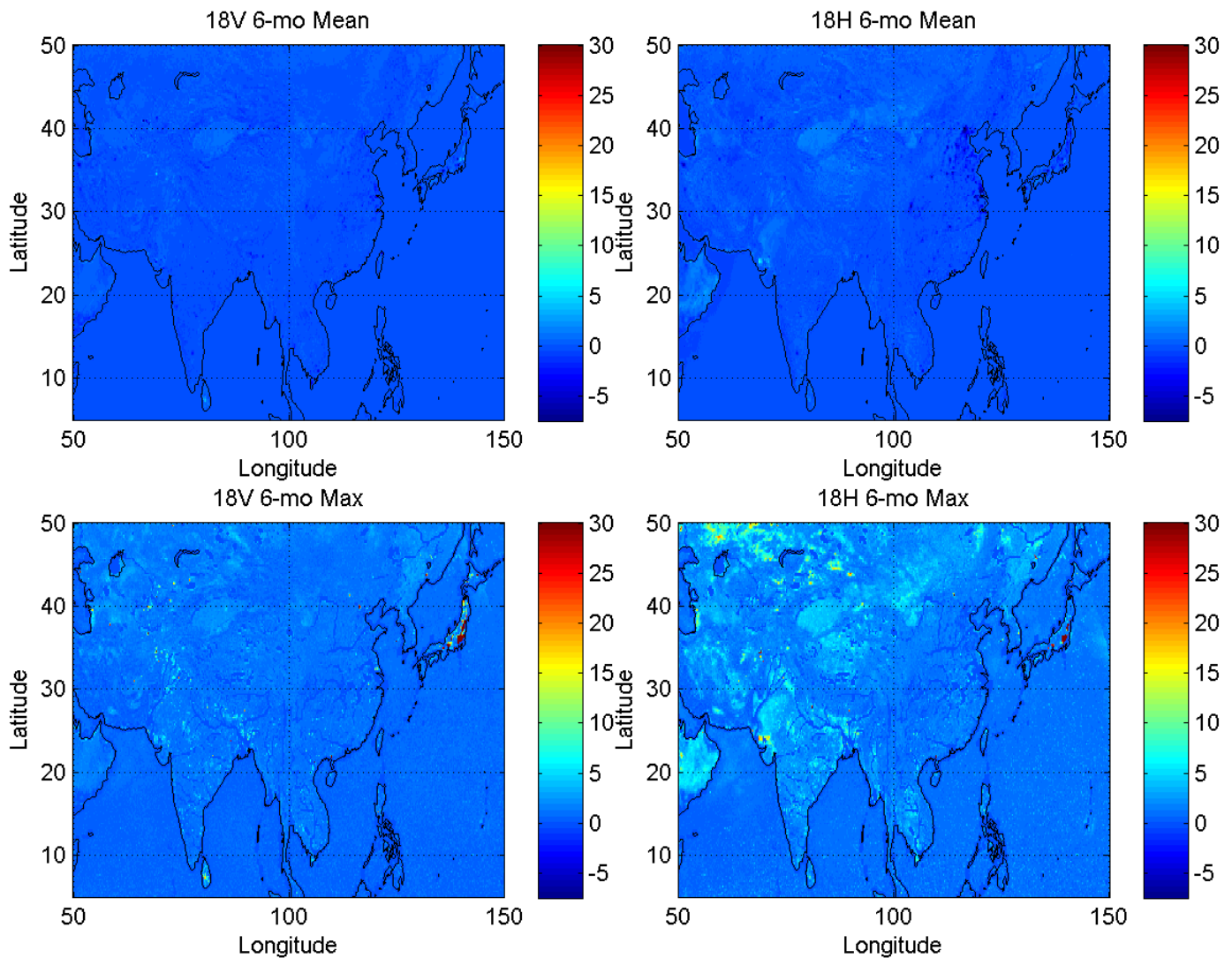


Figure 13. Asia 18 GHz RFI index over 6 months of data from March 2014 through September 2014. Top left: average v-pol RFI index. Top right: average h-pol RFI index. Bottom left: maximum daily average v-pol RFI index. Bottom right: maximum daily average h-pol RFI index. The H-pol channel is subject to higher geophysical variation, which increases the RFI index areas such as Russia and India.

~~Export or re-export of information contained herein may be subject to restrictions and requirements of U.S. export laws and regulations, and may require advance authorization from the U.S. Government~~

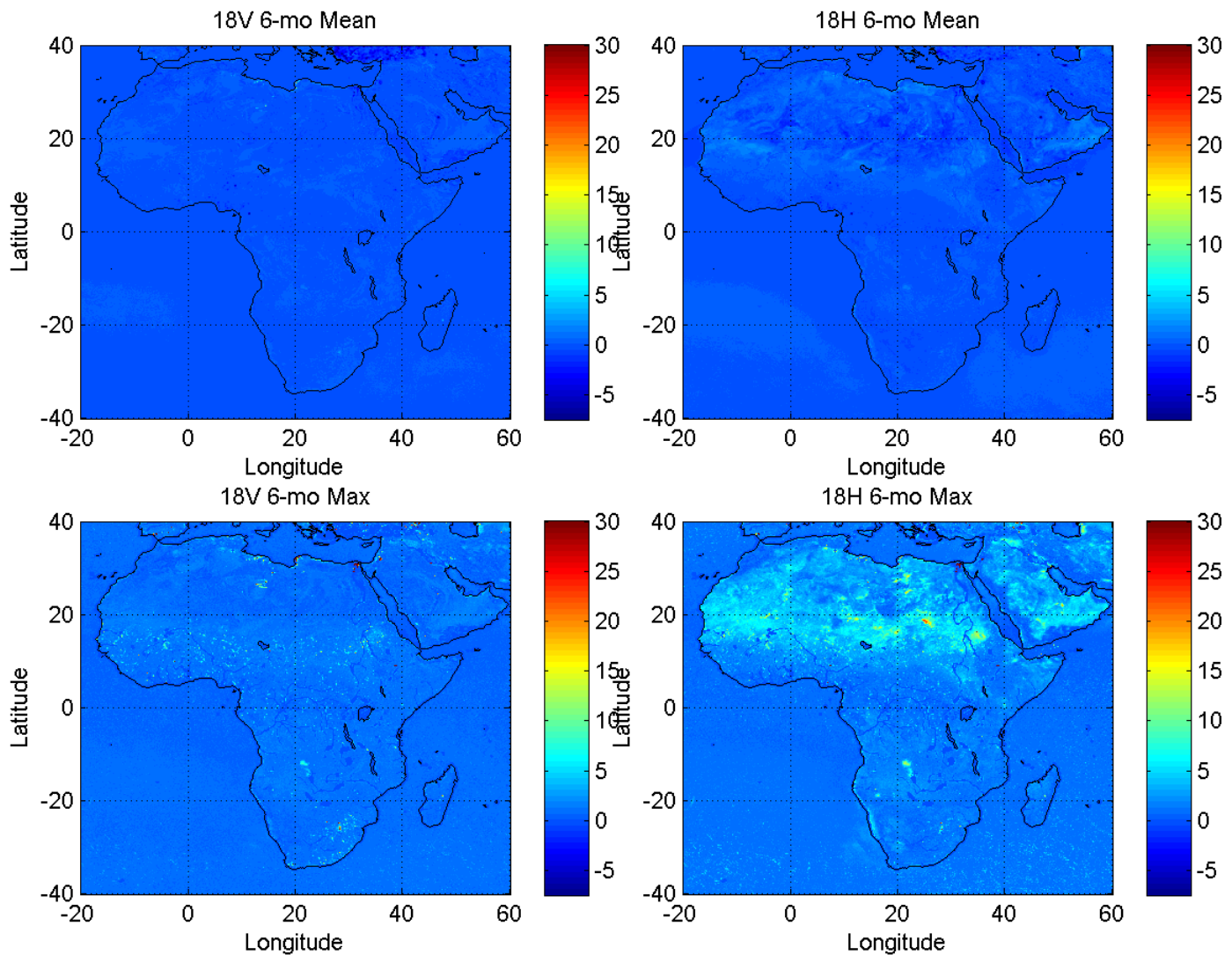


Figure 14. Africa 18 GHz RFI index over 6 months of data from March 2014 through September 2014. Top left: average v-pol RFI index. Top right: average h-pol RFI index. Bottom left: maximum daily average v-pol RFI index. Bottom right: maximum daily average h-pol RFI index. Libya exhibits the most 18 GHz RFI. The H-pol channel is subject to higher geophysical variation over the Sahara desert, which increases the RFI index.

Document No. 2444347Rev. A

Page

19

of

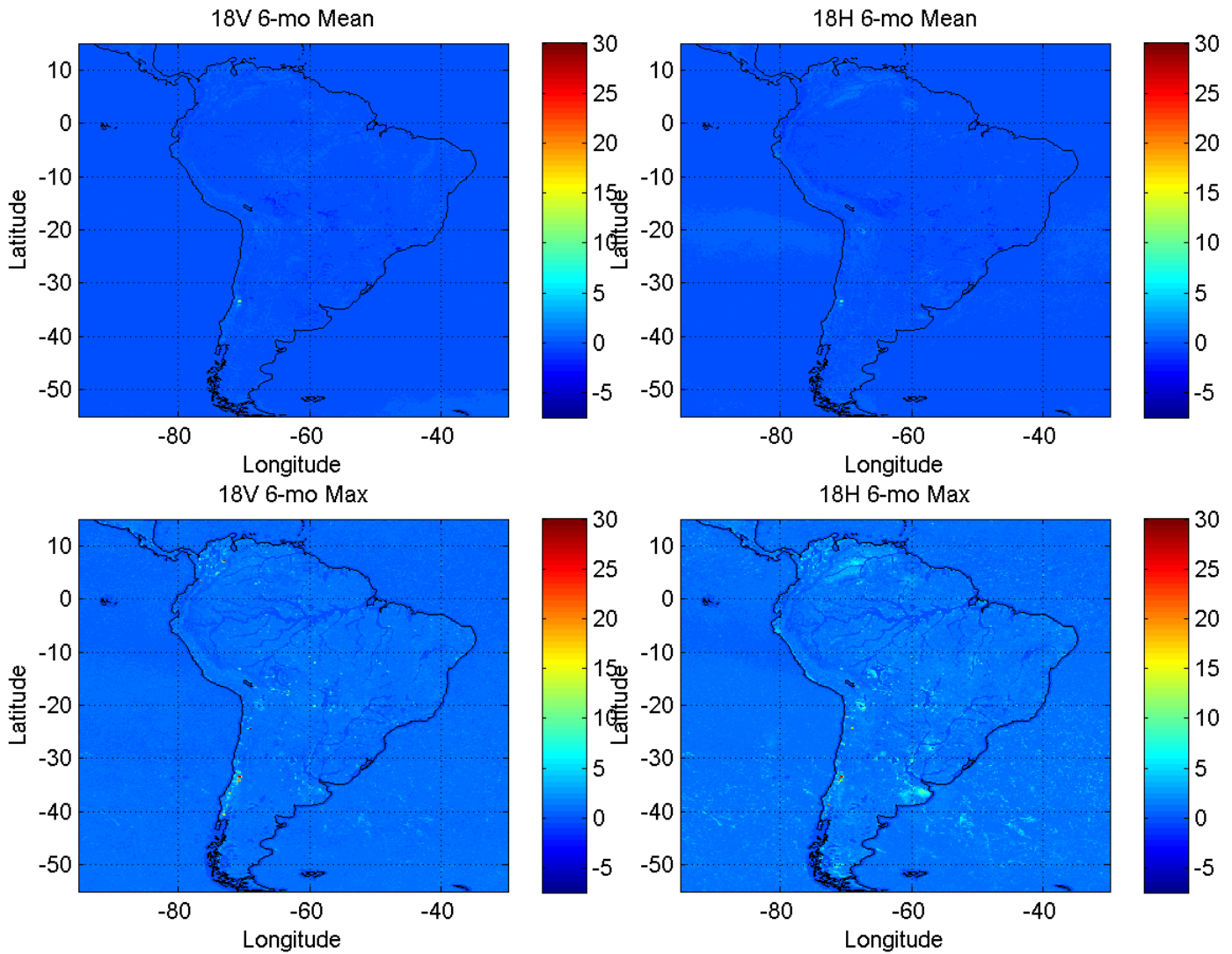
32

Figure 15. South America 18 GHz RFI index over 6 months of data from March 2014 through September 2014. Top left: average v-pol RFI index. Top right: average h-pol RFI index. Bottom left: maximum daily average v-pol RFI index. Bottom right: maximum daily average h-pol RFI index. Santiago Chile exhibits the highest RFI levels.

~~Export or re-export of information contained herein may be subject to restrictions and requirements of U.S. export laws and regulations, and may require advance authorization from the U.S. Government~~

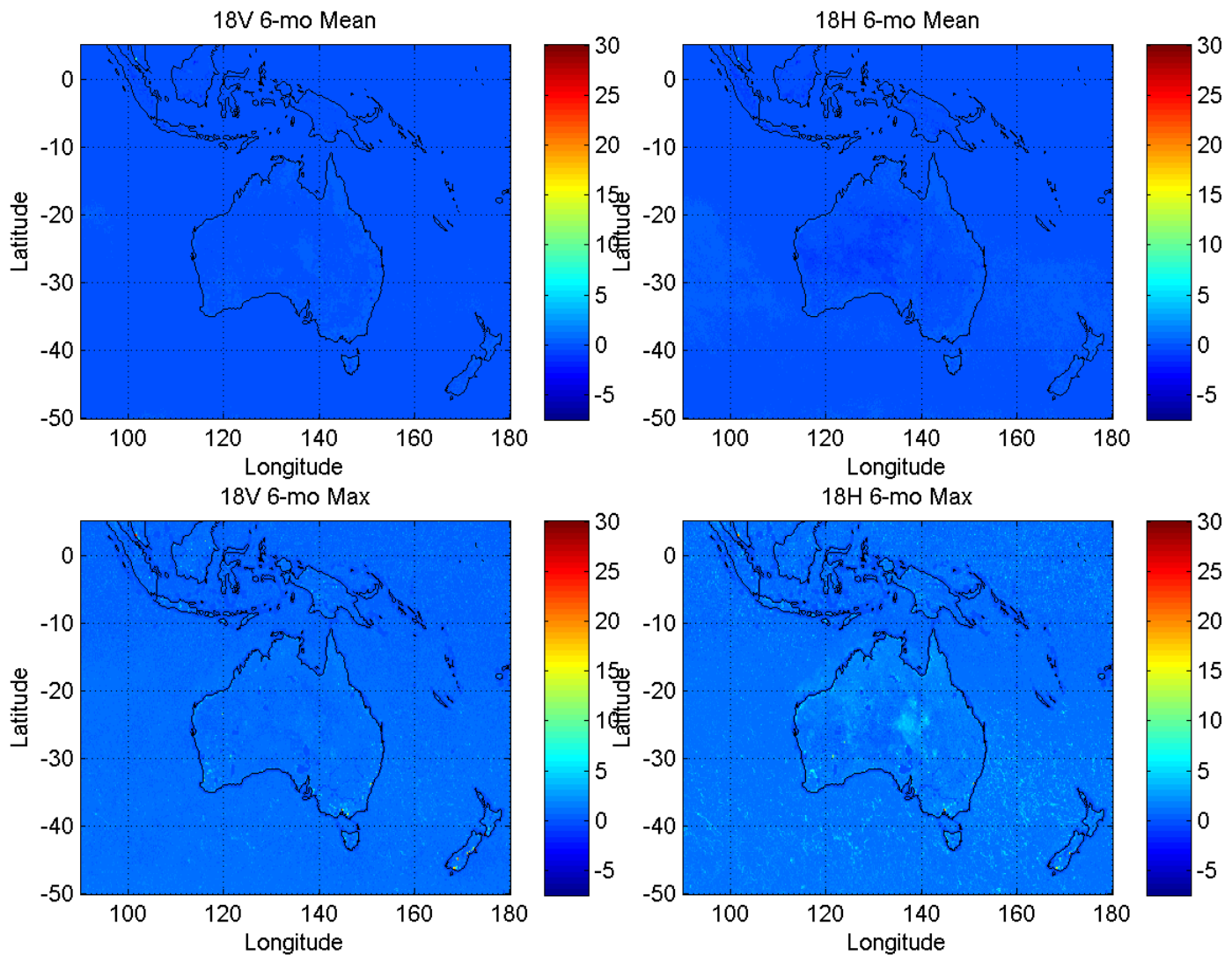


Figure 16. Australia 18 GHz RFI index over 6 months of data from March 2014 through September 2014. Top left: average v-pol RFI index. Top right: average h-pol RFI index. Bottom left: maximum daily average v-pol RFI index. Bottom right: maximum daily average h-pol RFI index.

~~Export or re-export of information contained herein may be subject to restrictions and requirements of U.S. export laws and regulations, and may require advance authorization from the U.S. Government~~



5.2 RFI from Direct Broadcast Satellites Reflecting off the Surface

The 18 GHz channels are affected by Earth/ocean surface reflections from geosynchronous satellites near the Great Lakes and ocean surrounding the continental US and Hawaii. The reflections are most noticeable over water, but are also noticed over land as well, likely reflecting off lakes (see Figure 17). The reflected RFI can be traced back to direct broadcast and internet satellites which utilize the GMI 18 GHz band for one-way earth-to-land transmission. In order to identify the particular satellites, the 18 GHz RFI index is projected to the location on the geosynchronous sphere where the satellites would need to be located in order that the transmitted signal would reflect off the Earth/ocean surface and enter into the main beam of the GMI antenna.

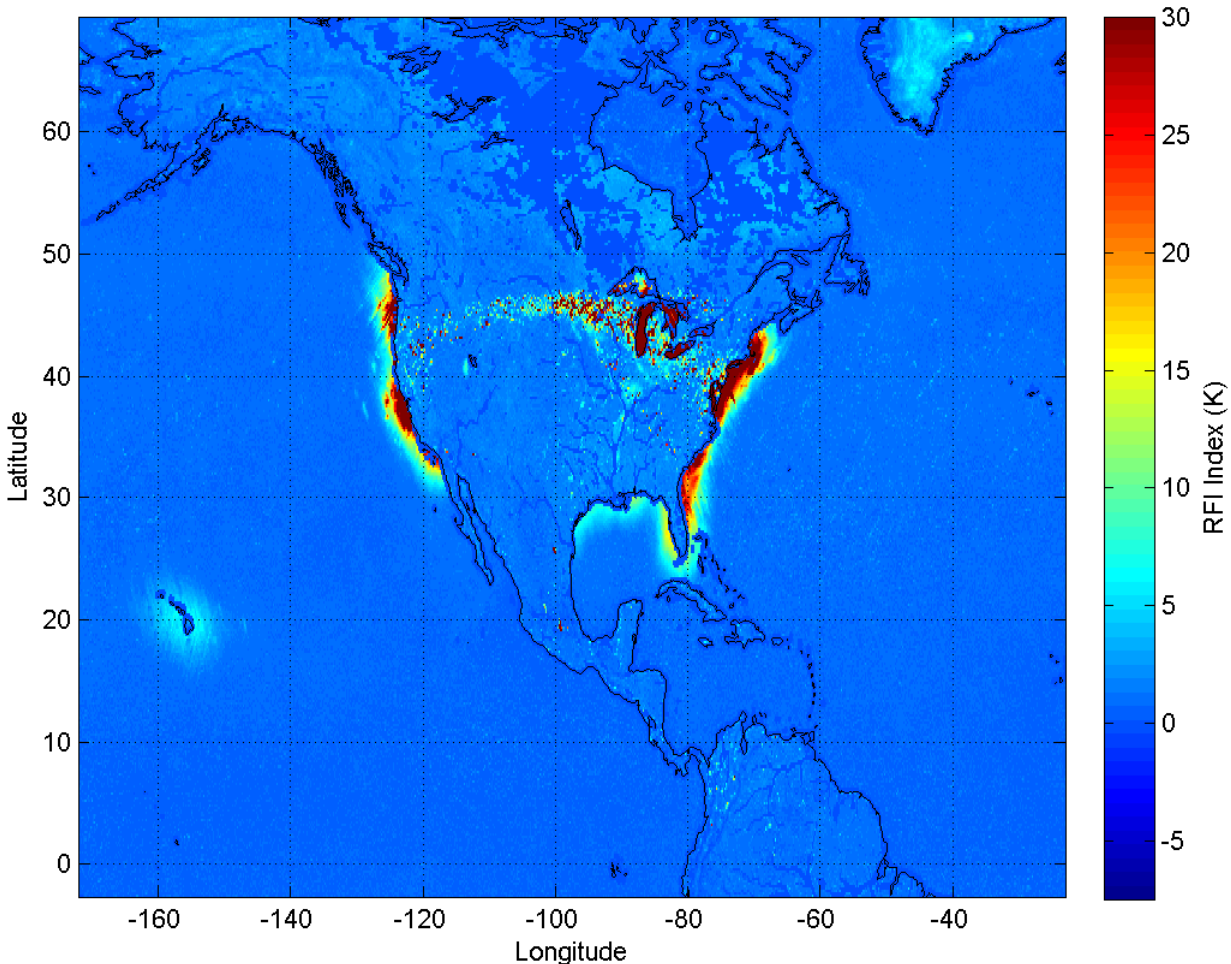


Figure 17. Maximum daily average 18V RFI index over North America and Hawaii from March to September 2014.

~~Export or re-export of information contained herein may be subject to restrictions and requirements of U.S. export laws and regulations, and may require advance authorization from the U.S. Government~~



Figure 18 shows the 18 GHz V-pol RFI index mapped to geosynchronous orbit through reflection off the earth surface. The most noticeable feature is the series of interference sources along the equatorial (geostationary) plane. The RFI is traced to satellites along the equatorial plane between -80 and -120 degrees longitude. Using public data available on the internet, the satellites corresponding to these source locations are determined and listed in Table 2.

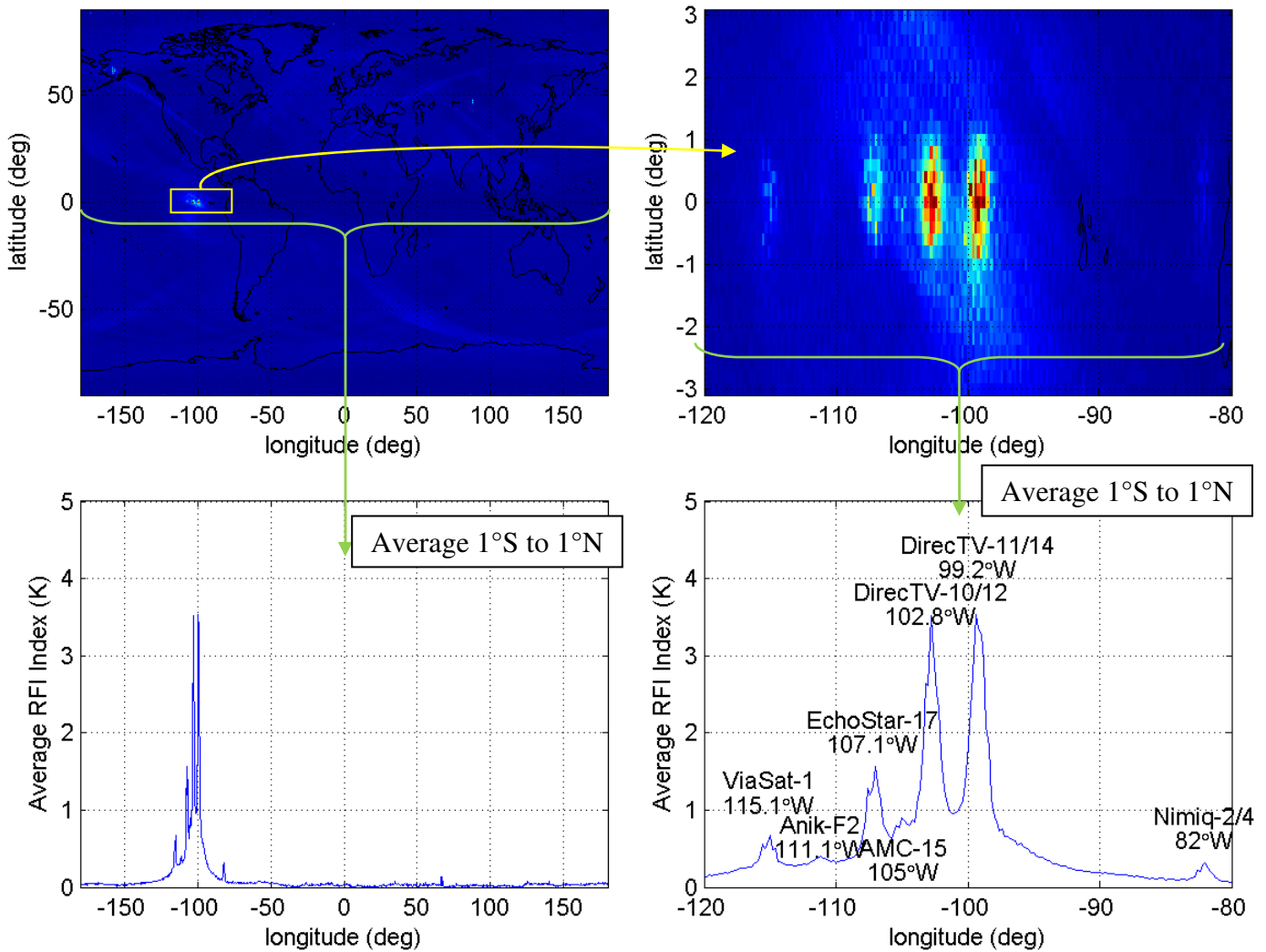


Figure 18. 18 GHz V-pol RFI index mapped through earth reflection to the distance of geosynchronous orbit. Top Left: All latitudes and longitudes. Top Right: Zoomed in to latitudes -3° to $+3^{\circ}$ and longitudes -120° to -80° . Bottom Left: Average of RFI index from -1° to $+1^{\circ}$ latitude for all longitudes. Bottom Right: Average RFI index from -1° to $+1^{\circ}$ latitude for longitudes -120° to -80° . Also listed in the lower right plot are the satellites with 18 GHz transmitters at the position of the interference sources.

Export or re-export of information contained herein may be subject to restrictions and requirements of U.S. export laws and regulations, and may require advance authorization from the U.S. Government


 Document No. 2444347 Rev. A Page 23 of 32
Table 2. Satellites assumed to interfere with the GMI 18 Ghz channels through reflection of transmitted signal off the earth/ocean surface.

Satellite Name	Operator	Orbital Position	Downlink Frequency Bands (GHz)	Function	Notes
ViaSat-1	Manx ViaSat IOM, ManSat, Telesat-IOM	115.1°W	18.3-19.3 19.7-20.2	High Speed Internet	1./2.
Anik-F2	Telesat Canada	111.1°W	3.7-4.2 11.7-12.2 17.8-18.3 18.3-18.8 19.7-20.2	Direct Broadcasting	2.
EchoStar-17	EchoStar Corp	107.1°W	18.3-18.8 18.8-19.3 19.7-20.2	High Speed Internet	2./3.
AMC-15	SES Americom	105.0°W	11.7-12.2 18.6-18.8 19.7-20.2	Direct Broadcasting	3./4.
DirecTV-10	DirecTV	102.8°W	18.3-18.8 19.7-20.2	Direct Broadcasting	4./5.
DirecTV-11	DirecTV	99.2°W	18.3-18.8 19.7-20.2	Direct Broadcasting	4./5.
DirecTV-12	DirecTV	102.8°W	18.3-18.8 19.7-20.2	Direct Broadcasting	4./5.
DirecTV-14	DirecTV	99.2°W	18.3-18.8 19.7-20.2	Direct Broadcasting	4./5.
Nimiq-2	Telesat Canada	82°W	17.8-18.3 18.3-18.8 19.7-20.2	Direct Broadcasting	2.
Nimiq-4	Telesat Canada	82°W	17.8-18.3 18.3-18.8 19.7-20.2	Direct Broadcasting	2.

1. See <http://www.spaceref.com/news/viewpr.html?pid=35059>
2. See <https://www.ic.gc.ca/eic/site/smt-gst.nsf/eng/sf02104.html#Note1>
3. See <http://www.n2yo.com/satellite/?s=38551>
4. See http://en.wikipedia.org/wiki/List_of_satellites_in_geosynchronous_orbit
5. See <http://en.wikipedia.org/wiki/DirecTV-10>

~~Export or re-export of information contained herein may be subject to restrictions and requirements of U.S. export laws and regulations, and may require advance authorization from the U.S. Government~~


 Document No. 2444347 Rev. A Page 24 of 32

5.3 RFI in the GMI Cold Swath

RFI events occur quite often in the GMI 10 and 18 GHz cold swaths. These events are due to direct intrusion of direct broadcasting and other internet or communication satellite signals into the GMI cold beams. They can be detected and removed using the RFI filtering technique described in BATC 2434007. The filtering technique provides a method to identify RFI events in the cold view over the first six months of on-orbit operations.

An example of RFI in the 10 GHz cold swath is shown in Figure 19.

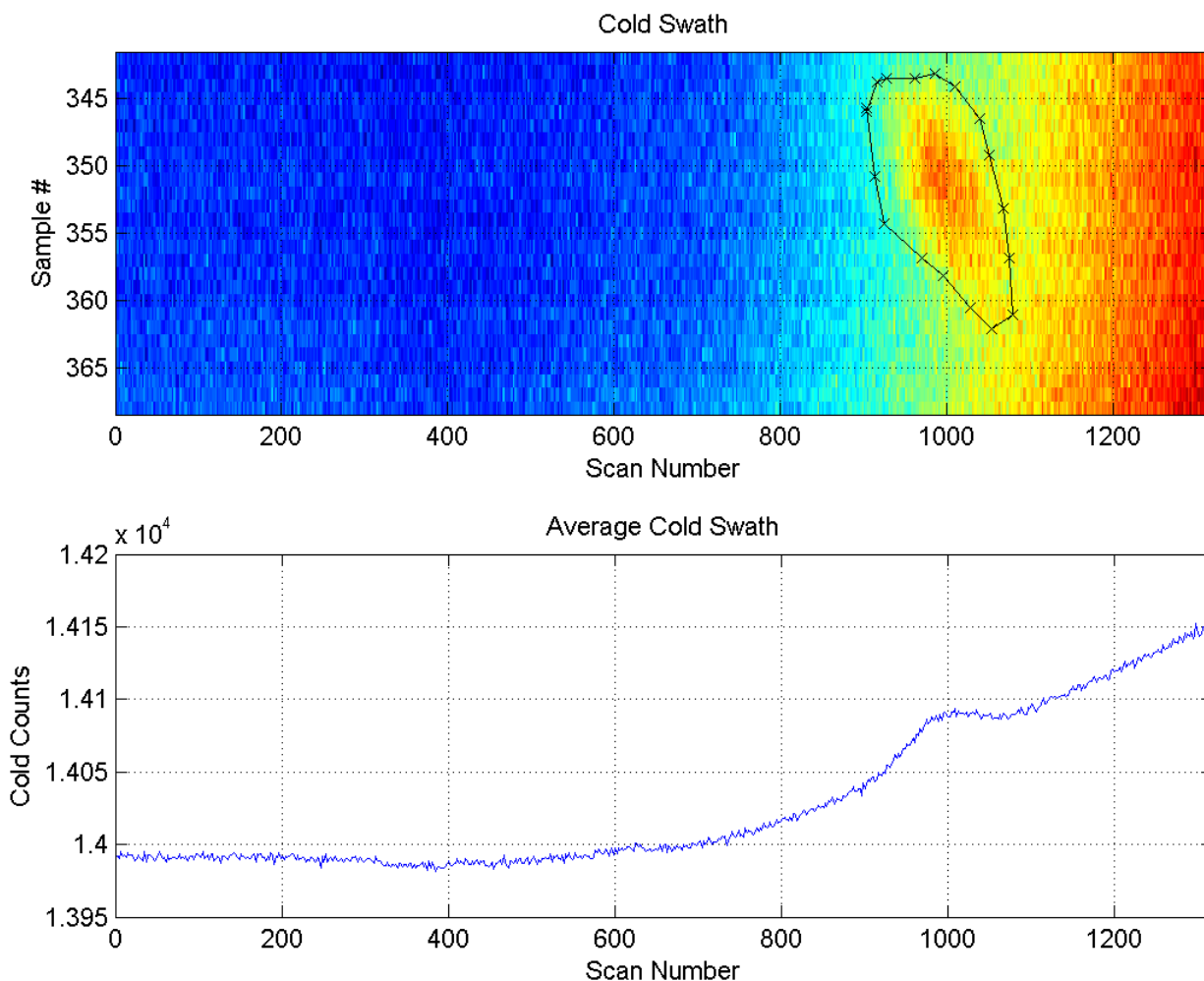


Figure 19. Cold swath example of RFI at 10 GHz.

~~Export or re-export of information contained herein may be subject to restrictions and requirements of U.S. export laws and regulations, and may require advance authorization from the U.S. Government~~

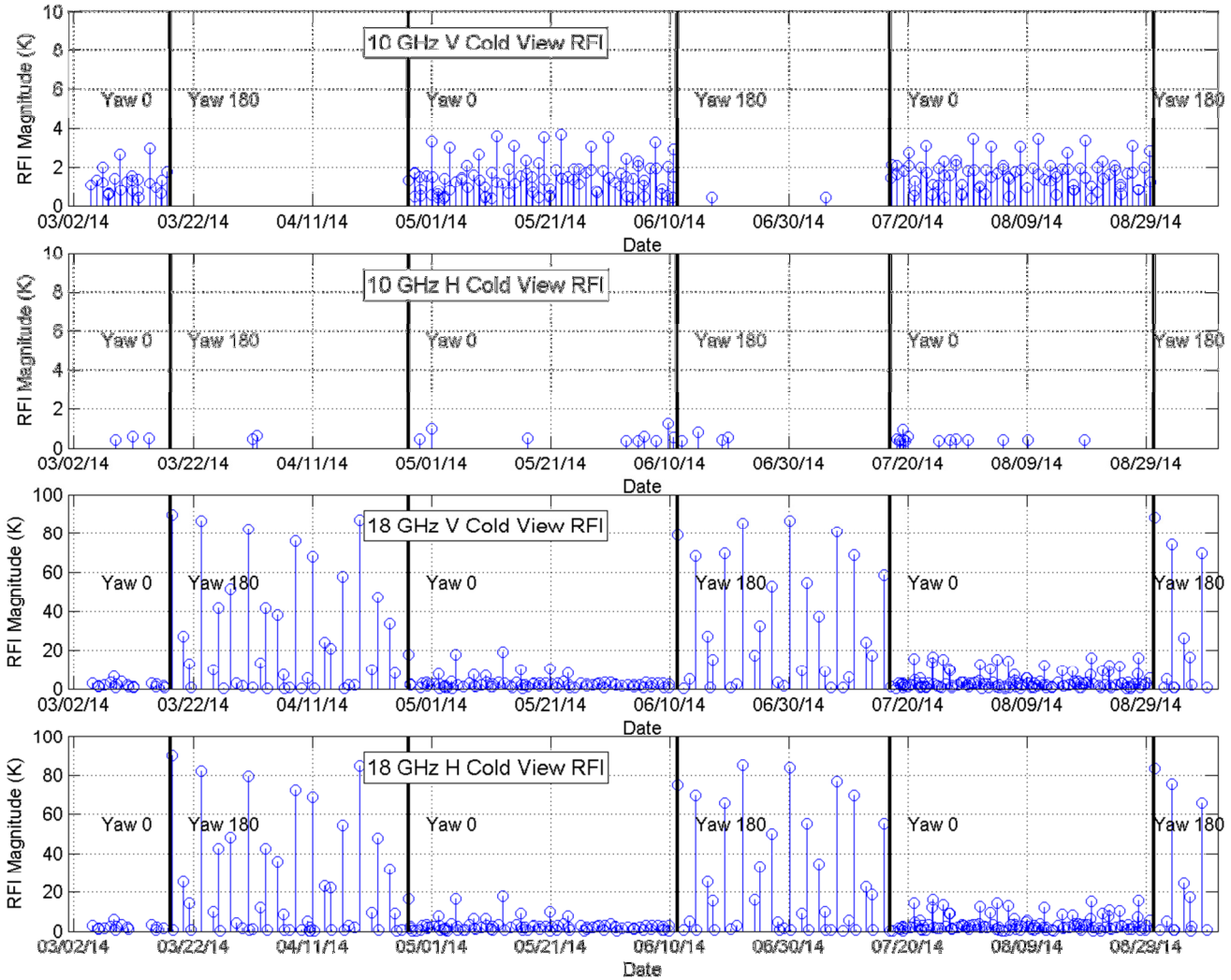


Figure 20. Peak RFI in the GMI cold swath detected by the cold swath RFI detection algorithm for the GMI 10 and 18 GHz channels. Notice the scale difference between the 10 and 18 GHz channel plots.

Figure 20 shows the peak RFI magnitude in the GMI cold swath for the 10 and 18 GHz channels as a function of time. We note that the actual impact of these RFI hits on the unfiltered cold swath is probably about 10% to 30% of the peak magnitude after averaging over the swath and over multiple scans. The largest RFI occurs at 18 GHz when the spacecraft is in the “180 degree yaw” orientation. All other 18 GHz RFI is within 20K, and mostly at “0 degree yaw”. Almost all the 10 GHz RFI occurs on the vertical polarization channel and at the 0 degree yaw orientation.

~~Export or re-export of information contained herein may be subject to restrictions and requirements of U.S. export laws and regulations, and may require advance authorization from the U.S. Government~~



In order to understand the sources of the cold swath RFI, the cold sky beam was projected out to the geosynchronous orbital sphere for each cold RFI incident as shown in Figure 21. The expected geosynchronous source location and the GPM core satellite location during the cold swath interference are shown in Figure 21. The size of the markers indicates the relative magnitude of the RFI. The large 18 GHz RFI that occurs at yaw 180 originates from satellites around 100°W transmitting to Hawaii. Smaller 18 GHz RFI events occur while the GMI is over Canada, Eastern Europe and Australia. Most of the 10 GHz RFI occurs while GMI is over Northern Europe. The suspected geosynchronous satellites causing the cold-swath interference are listed in Table 3.

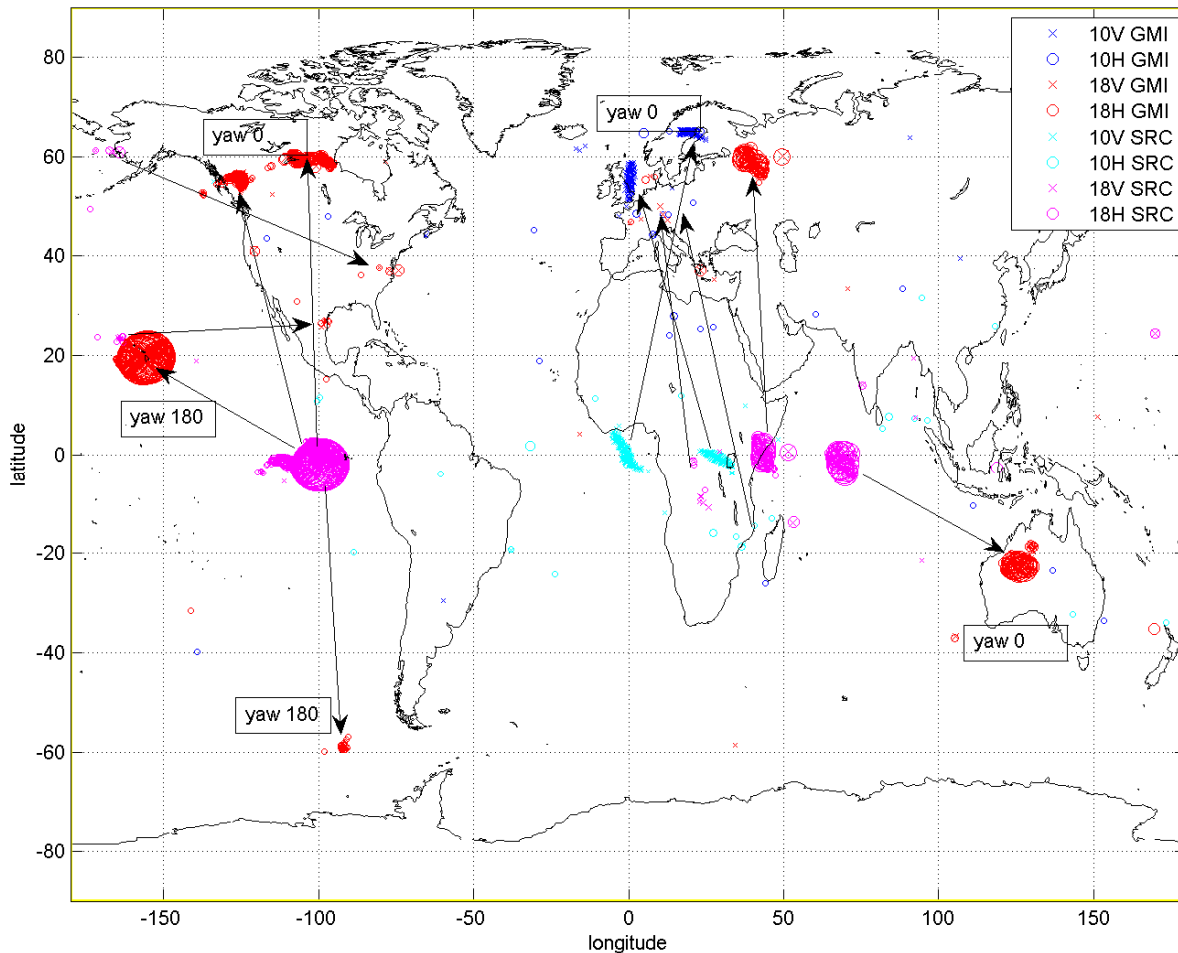


Figure 21. RFI source locations (cyan and magenta) at geosynchronous distance from the earth and location of the GMI (blue and red) for each cold swath RFI. The size of the markers indicate the relative magnitude of the RFI.

~~Export or re-export of information contained herein may be subject to restrictions and requirements of U.S. export laws and regulations, and may require advance authorization from the U.S. Government~~


 Document No. 2444347 Rev. A Page 27 of 32
Table 3. Likely satellites for cold-view RFI as shown in Figure 21.

Satellite Name	Operator	Orbital Position	Downlink Frequency Bands (GHz)	Function	Notes
(See Table 2)	(Multiple)	82°W – 115.1°W	(Multiple)	Direct Broadcasting / High Speed Internet	Table 1 lists possible western hemisphere interferers
Thor-6	Telnor Sat (Norway /Sweden)	0.8°E	10.716-12.456	Direct Broadcasting	1.
Astra 2D/E	SES S.A.	28.5°E	10.714-12.480	Direct Broadcasting	1.
Unknown	Unknown	43.2°E	Unknown	Unknown	2.
Intelsat 7 Intelsat 20 (TBR)	Intelsat	68.5°E	3.7-4.2 10.95-12.75 19.7-20.2	Direct Broadcasting	3.

1. <http://en.kingofsat.net/sat-thor6.php>
2. Unable to find information about satellites at this position. This satellite appears to illuminate Russia. The interference for this satellite began between 6/11/2014 and 7/17/2014.
3. <http://www.flysat.com/is20-info.php>. This satellite does not transmit directly in the GMI 18 GHz band. interference possibly caused by a 5th-harmonic from one of the C-band channels, or from a different satellite not listed on publically available sites.

6 SUMMARY

This paper presents the results of an RFI study for the GMI. The RFI detection method is based on the assumption that earth-based signals over land and ocean have predictable spectral correlations that can be exploited to identify RFI in a channel of interest compared to a linear combination of other channels of different center frequencies. RFI is prevalent only in the 10.65 and 18.7 GHz channels. No other channels have evidenced RFI. The 10 GHz RFI is mainly ground-based with high levels of RFI in Europe and parts of Asia and Africa. Ground based RFI exists in the 18 GHz channel in specific countries. The 18 GHz channels detect RFI from reflections from direct broadcasting satellites off the Great Lakes and oceans surrounding the continental United States and Hawaii. Both the 10 and 18 GHz channels exhibit RFI in the cold sky swath from geosynchronous direct broadcasting and internet satellites.

7 FUTURE WORK

This document describes and RFI flagging method for 10 and 18 GHz. If need be, the method can be expanded to other channels. Also, the 10 GHz channel flag requires quite high thresholds for native resolution files. More work could be done to improve the flagging capability of the algorithm for the 10 GHz channels.

~~Export or re-export of information contained herein may be subject to restrictions and requirements of U.S. export laws and regulations, and may require advance authorization from the U.S. Government~~


 Document No. 2444347 Rev. A Page 28 of 32

8 APPENDIX A: Generalized RFI Index Coefficients

Channel/Surface	a'[10V]	a'[10H]	a'[18V]	a'[18H]	a'[23V]	a'[36V]	a'[36H]	a'[89V]	a'[89H]	b'[10V]	b'[10H]	b'[18V]	b'[18H]	b'[23V]	b'[36V]	b'[36H]	b'[89V]	b'[89H]	a'o
10 GHz V Land	1	0	-5.097	-0.164	7.2372	-3.443	0.8798	1.5534	-1.302	0	0	0.00557	0.00053	-0.0121	0.00749	-0.0021	-0.0034	0.0028	-87.17
10 GHz V Ocean	1	0	-4.299	0.9851	0.0953	1.9043	-0.606	-0.436	0.0739	0	0	0.0048	-0.0012	0.00075	-0.0017	0.0004	0.00068	-0.0001	131.75
10 GHz V Sea Ice	1	0	-4.531	-2.279	10.464	-5.22	3.902	2.1779	-3.607	0	0	0.00596	0.0049	-0.0206	0.01165	-0.0086	-0.0046	0.00798	-265.9
10 GHz H Land	0	1	-5.039	-0.654	7.1952	-4.101	1.7079	2.4863	-2.165	0	0	0.00838	-0.002	-0.0118	0.00739	-0.0021	-0.0054	0.00465	-52.23
10 GHz H Ocean	0	1	-1.257	-0.288	-0.281	-0.721	-0.071	0.0602	0.1554	0	0	-0.0003	-0.0001	0.0022	0.00384	-0.0007	-0.0002	-0.0004	142.98
10 GHz H Sea Ice	0	1	3.6806	-2.466	0.158	-0.896	1.7923	0.9677	-1.564	0	0	-0.0108	0.00232	0.00401	0.00078	-0.0026	-0.0019	0.00338	-352.5
18 GHz V Land	0.2472	-0.332	1	0	-1.927	1.5738	-0.088	-0.781	0.4015	-0.001	0.00067	0	0	0.00224	-0.003	5E-05	0.00155	-0.0007	-14.18
18 GHz V Ocean	1.0453	-0.118	1	0	0.1811	-0.699	0.0161	1.3054	-0.383	-0.0042	0.0004	0	0	-0.0013	0.00112	-0.0003	-0.0027	0.00108	-243.9
18 GHz V Sea Ice	0.2373	0.0386	1	0	-2.398	1.1116	-0.517	-1.061	1.2183	-0.0012	8E-05	0	0	0.00326	-0.0019	0.00077	0.00203	-0.0024	53.2
18 GHz H Land	0.8158	-0.955	0	1	-1.509	2.4864	-1.364	-1.192	0.9413	-0.0012	0.00114	0	0	0.00125	-0.0031	0.00087	0.0019	-0.0013	-31.72
18 GHz H Ocean	0.2869	0.1553	0	1	0.2403	1.6059	-0.769	1.5384	-0.531	-0.0003	-0.0036	0	0	-0.0021	-0.0023	0.00032	-0.0034	0.00164	-361.8
18 GHz H Sea Ice	0.1461	-0.3	0	1	-1.237	1.1453	-1.381	-0.993	0.9364	8.9E-05	-0.0003	0	0	0.00069	-0.0003	0.001	0.00155	-0.0015	84.528

~~Export or re-export of information contained herein may be subject to restrictions and requirements of U.S. export laws and regulations, and may require advance authorization from the U.S. Government~~



Document No. 2444347 Rev. A Page 29 of 32

9 Appendix B: Earth RFI Location Database

The RFI index for each 10 and 18 GHz channel has been compiled over a 0.2 degree grid, and can be found in the data file gmi_earth_rfi_map.mat. For each grid point where the RFI index map shows an RFI peak above a threshold, the nearest city to the RFI peak has been identified. The locations of each RFI peak and the nearest city are given in the associated spreadsheet 2444347-GMI_RFI_SS15_RFIdatabase.xlsx and shown in the tables below.

~~Export or re-export of information contained herein may be subject to restrictions and requirements of U.S. export laws and regulations, and may require advance authorization from the U.S. Government~~



Ball Aerospace & Technologies Corp.

Systems Engineering Report

1600 Commerce Street Boulder, Colorado 80301

Document No. 2444347

Rev. A

Page 30 of 32

10 GHz V-pol RFI Locations

Table with 5 columns: Lat (deg), Lon (deg), Mean (K), Max (K), Location. Lists various RFI locations across the United States and Mexico.

Table with 5 columns: Lat (deg), Lon (deg), Mean (K), Max (K), Location. Lists various RFI locations across Europe, Africa, and the Middle East.

Table with 5 columns: Lat (deg), Lon (deg), Mean (K), Max (K), Location. Lists various RFI locations across Asia, Australia, and the Pacific region.

Table with 5 columns: Lat (deg), Lon (deg), Mean (K), Max (K), Location. Lists various RFI locations across South America, Africa, and the Middle East.

Export or re-export of information contained herein may be subject to restrictions and requirements of U.S. export laws and regulations, and may require advance authorization from the U.S. Government

Vertical text on the right edge: Lifecycle: Rev Release Date: 1/19/2015 12:34:02 PM

System Engineering Report: 2444347 Program: GMI



Ball Aerospace & Technologies Corp.

Systems Engineering Report

1600 Commerce Street Boulder, Colorado 80301

Document No. 2444347

Rev. A

Page 31

of 32

10 GHZ H-pol RFI Locations

Table with columns: Lat (deg), Lon (deg), Mean (K), Max (K), Location. Lists various RFI locations across North America, Europe, and Asia.

Table with columns: Lat (deg), Lon (deg), Mean (K), Max (K), Location. Continues the list of RFI locations from the previous table.

Table with columns: Lat (deg), Lon (deg), Mean (K), Max (K), Location. Continues the list of RFI locations from the previous table.

Table with columns: Lat (deg), Lon (deg), Mean (K), Max (K), Location. Continues the list of RFI locations from the previous table.

Export or re-export of information contained herein may be subject to restrictions and requirements of U.S. export laws and regulations, and may require advance authorization from the U.S. Government

Lifecycle: Production Released Rev Release Date: 1/19/2015 12:34:02 PM



Table with 2 main sections: '18 GHz V-pol RFI Locations' and '18 GHz H-pol RFI Locations'. Each section contains columns for Lat (deg), Lon (deg), Mean (K), Max (K), and Location. The locations include various international sites such as Budzlaika, Belarus; Johannesburg, South Africa; Prusy, Belarus; Zhytkavichy, Belarus; Sasnovy, Belarus; Kosary, Belarus; Borisov, Belarus; Berezino, Belarus; Lepel, Belarus; Polatsk, Belarus; Kotly, Belarus; Babrusjsk, Belarus; Krupki, Belarus; Krasnapolle, Belarus; Senno, Belarus; Petrovskoye, Belarus; Haradok, Belarus; El Obeid, Sudan; Vitebsk, Belarus; Bykhaw, Belarus; Mahilyow, Belarus; Orsha, Belarus; Saint Petersburg, Russia; Liozna, Belarus; Gomel, Belarus; Smolensk, Russia; Al Qadarif, Sudan; Kaluga, Russia; Tokat, Turkey; Moscow, Russia; Andohalo, Madagascar; Ruwais, United Arab Emirates; Dubai, United Arab Emirates; Heart, Afghanistan; Karachi, Pakistan; Masari Sharif, Afghanistan; Kabul, Afghanistan; Karagandy, Pakistan; Gujrandwala, Pakistan; Lahore, Pakistan; Novyabrsk, Russia; Almaty, Kazakhstan; Colombo, Sri Lanka; Pitigala, Sri Lanka; Avissawella, Sri Lanka; Matale, Sri Lanka; Kuala Lumpur, Malaysia; Irkutsk, Russia; Phnom Penh, Cambodia; Ulan-Ude, Russia; Beijing, China; Nihonmatsu, Japan; Koga, Japan; Yuzhno-Sakhalinsk, Russia.

Export or re-export of information contained herein may be subject to restrictions and requirements of U.S. export laws and regulations, and may require advance authorization from the U.S. Government



**Ball Aerospace
& Technologies Corp.**

P.O. Box 1062
Boulder, CO 80306

PART OR ALL OF EO RELEVANT TO SPECIFIC DOCUMENT INFORMATION ONLY

ENGINEERING ORDER - STANDARD

SHEET 1 of 1

CHANGE NO. C446818

STATUS Released

ORIGINATOR AND DATE Draper, David 01/19/2015

CAGE 13993

ATTACHMENT(S): NO Note: THIS ORDER IS NOT COMPLETE WITHOUT ATTACHMENT(S) IF "ATTACHMENT" IS INDICATED

REASON FOR CHANGE: Initial Release

DESCRIPTION OF CHANGE: 2444347 (A) REPORT ON GMI SPECIAL STUDY #15: RADIO FREQUENCY INTERFERENCE

AFFECTED ITEMS

PART NO.	REV (OLD)	LIFECYCLE OLD	NOMENCLATURE	REV (NEW)	LIFECYCLE NEW	DISPOSITION	CII's
2444347			REPORT ON GMI SPECIAL STUDY #15: RADIO FREQUENCY INTERFERENCE	A	Production Released	Not Applicable	IN001A

CHANGE CLASS Initial Release

CHANGE CODE

DWG TITLE

REPORT ON GMI SPECIAL STUDY #15: RADIO FREQUENCY INTERFERENCE...

DWG NO 2444347

NEW A REV

Status: Released